RadioGraphics

From the Archives of the AFIP

Imaging of Primary Chondrosarcoma: Radiologic-Pathologic Correlation[1]

CME FEATURE

See accompanying test at http://www.rsna.org/education/rg_cme.html

LEARNING OBJECTIVES FOR TEST 6

After reading this article and taking the test, the reader will be able to:

- List the radiologic spectrum of primary chondrosarcoma.
- Describe the pathologic basis of the radiologic features of primary chondrosarcoma.
- Recognize the radiologic manifestations that may allow differentiation of the various types of primary chondrosarcoma.

Mark D. Murphey, MD • Eric A. Walker, MD • Anthony J. Wilson, MB, ChB • Mark J. Kransdorf, MD • H. Thomas Temple, MD • Francis H. Gannon, MD

Chondrosarcoma is a malignant tumor that produces cartilage matrix, and lesions that arise de novo are called primary. Primary chondrosarcoma is the third most common primary malignant tumor of bone, constituting 20%–27% of all primary malignant osseous neoplasms. There are numerous types of primary chondrosarcomas, including conventional intramedullary, clear cell, juxtacortical, myxoid, mesenchymal, extraskeletal, and dedifferentiated. The conventional intramedullary chondrosarcoma is the most frequent type, and it most commonly involves the long bones or pelvis in up to 65% of cases. Although the pathologic appearance varies with specific lesion type, chondrosarcomas grow with lobular type architecture, and these hyaline cartilage nodules demonstrate high water content and peripheral enchondral ossification. Imaging features directly reflect this pathologic appearance, and the various subtypes often show distinctive features. Radiographic findings often suggest the diagnosis of chondrosarcoma because of identification of typical "ring-and-arc" chondroid matrix mineralization (representing the enchondral ossification) and aggressive features of deep endosteal scalloping and soft-tissue extension. These latter features are usually best assessed, as is lesion staging, with computed tomography (CT) or magnetic resonance (MR) imaging. CT is optimal to detect the matrix mineralization, particularly when it is subtle or when the lesion is located in anatomically complex areas. Both CT and MR imaging depict the high water content of these lesions as low attenuation and very high signal intensity with T2-weighting, respectively. Understanding and recognizing the spectrum of appearances of the various types of primary chondrosarcoma allow improved patient assessment and are vital for optimal clinical management including diagnosis, biopsy, staging, treatment, and prognosis.

Index terms: Bone neoplasms, 40.321 • Bone neoplasms, CT, 40.1211 • Bone neoplasms, MR, 40.12141 • Sarcoma, 40.321

RadioGraphics 2003; 23:1245–1278 • **Published online** 10.1148/rg.235035134

[1]From the Departments of Radiologic Pathology (M.D.M., E.A.W., A.J.W.) and Orthopedic Pathology (F.H.G.), Armed Forces Institute of Pathology, 6825 16th Street NW, Bldg 54, Rm M-133A, Washington, DC 20306; Departments of Radiology and Nuclear Medicine, Uniformed Services University of the Health Sciences, Bethesda, Md (M.D.M.); Department of Radiology, University of Maryland School of Medicine, Baltimore (M.D.M.); Department of Radiology, Harborview Medical Center, Seattle, Wash (A.J.W.); Department of Radiology, Mayo Clinic, Jacksonville, Fla (M.J.K.); and Department of Orthopedic Surgery, University of Miami School of Medicine, Miami, Fla (H.T.T.). Received May 19, 2003; revision requested June 10 and received June 20; accepted June 23. **Address correspondence to** M.D.M. (e-mail: *murphey@afip.osd.mil*).

Introduction

Chondrosarcoma is a malignant tumor with cells that produce cartilage matrix. Chondrosarcomas that arise de novo are called primary chondrosarcomas. Conversely, chondrosarcomas superimposed on preexisting benign cartilaginous neoplasms such as enchondroma or osteochondroma are referred to as secondary chondrosarcomas. Chondrosarcomas are also categorized as central, peripheral, or juxtacortical (periosteal) lesions depending on their osseous location. Central chondrosarcomas are intramedullary in origin, although large tumors may erode the cortex and invade the surrounding soft tissue. Peripheral chondrosarcomas are subdivided into those secondary to a preexisting osteochondroma and those developing from the bone surface (juxtacortical).

Chondrosarcoma is the third most common primary malignant tumor of bone, exceeded in frequency only by multiple myeloma and osteosarcoma. Chondrosarcoma accounts for 3.5% of all primary bone tumors that lead to biopsy and 20%–27% of primary malignant osseous neoplasms (1–7).

Numerous categories (incorporating both location and histologic characteristics) of primary chondrosarcomas have been described, including conventional intramedullary, clear cell, juxtacortical, myxoid, mesenchymal, extraskeletal, and dedifferentiated. Radiographic findings often strongly suggest the diagnosis of chondrosarcoma by demonstrating a lesion with typical chondroid matrix mineralization (ring-and-arc pattern) and aggressive growth features. Additional imaging modalities including bone scintigraphy, computed tomography (CT), and magnetic resonance (MR) imaging are frequently employed to evaluate these neoplasms further and for purposes of staging and guiding surgical resection. In this article, the clinical characteristics, pathologic features, various radiologic appearances, and treatment and prognosis for the different types of primary chondrosarcoma are discussed and illustrated.

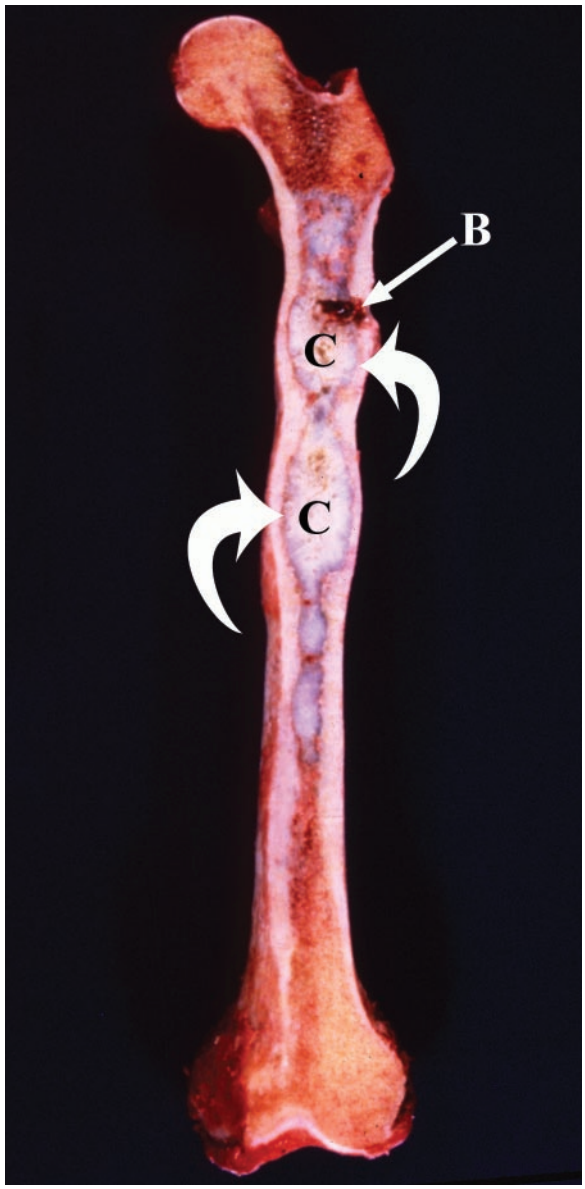

Figure 1. Photograph of a coronally sectioned gross specimen of a conventional intramedullary chondrosarcoma of the femur demonstrates a multilobulated lesion replacing a long extent of the marrow space *(C)*. Two foci of deep endosteal scalloping (greater than two-thirds of the normal cortical thickness) with expansile remodeling of bone (arrows) are seen. A biopsy site is noted at the superolateral diaphysis *(B)*.

Pathologic Features

Conventional Intramedullary Chondrosarcoma

At gross pathologic evaluation, conventional intramedullary chondrosarcomas are large lesions, the majority being greater than 4 cm in size (1–7). In fact, in one study, 50% of chondrosarcomas were greater than 10 cm in size, occupying from 30% to more than 50% of the bone length (Fig 1) (8). These hyaline cartilage neoplasms typically grow with a lobular architecture (Figs 1, 2). This growth pattern frequently causes lobular, deep, endosteal scalloping that may result in focal areas of cortical penetration and associated soft-tissue extension. Nonmineralized regions have a translucent appearance, reflecting the high water content of hyaline cartilage, particularly in low-grade lesions. Areas with matrix mineralization (calcification) appear granular and gritty in consistency.

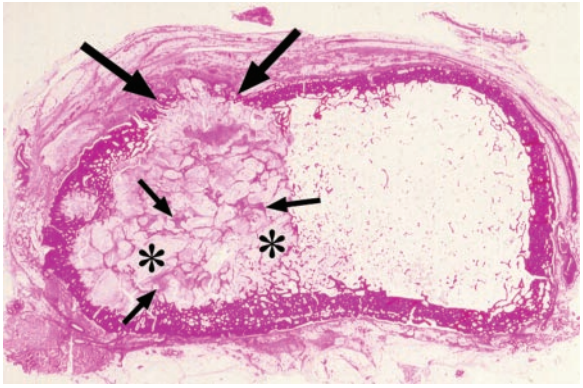

Figure 2. Photograph of an axially sectioned whole-mounted specimen (hematoxylin-eosin stain) shows multiple cartilaginous lobules (*) replacing the femoral marrow with deep endosteal scalloping anteriorly, cortical penetration, and a small focus of soft-tissue extension (large arrows), findings that represent conventional intramedullary chondrosarcoma. Enchondral ossification at the periphery of the chondroid lobules causing a ring-and-arc appearance is also seen (small arrows).

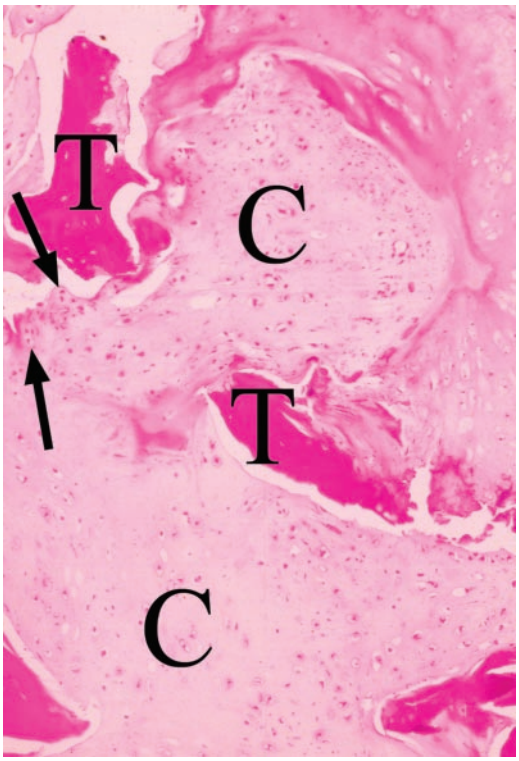

Figure 3. High-power photomicrograph (original magnification, ×200; hematoxylin-eosin stain) shows a grade 2 conventional chondrosarcoma with cartilage lobules *(C)* entrapping osseous trabeculae *(T)* and cellular atypia represented by multinucleated cartilage cells (arrows).

Histologic examination reveals lobules of hyaline cartilage (Figs 1, 2). The areas of matrix mineralization associated with conventional intramedullary chondrosarcoma have a distinctive ring-and-arc–like pattern. This pattern reflects enchondral ossification around lobules of well-formed hyaline cartilage (Fig 2). Higher-grade chondrosarcomas have larger areas that are not calcified. The nonmineralized tissue in chondrosarcoma has high water content, varying histologically from mature hyaline cartilage to a more myxoid stroma. The single most important feature distinguishing conventional intramedullary chondrosarcoma from enchondroma is the relationship of the chondroid tissue to the surrounding bone (2,3). Entrapment and destruction of the surrounding trabecular bone is the hallmark of a chondrosarcoma and should be identified before conclusively making this diagnosis (Fig 3). Sections taken at the edge of conventional intramedullary chondrosarcoma best demonstrate cartilage invading the marrow between trabecular bone (1–5). Once this morphologic feature has been identified, the degree of cellularity is used to determine grading (see later discussion). Most of the host bone is resorbed, but partially replaced trabeculae may become completely surrounded by proliferating cartilage, remaining as islands of normal bone within the neoplasm. Invasion and resorption of the cortex, beginning with the endosteal surface, occur as the first step in extraosseous extension.

The broad microscopic spectrum seen with conventional intramedullary chondrosarcomas lends itself to histologic grading and correlates with the clinical behavior of these lesions and their ultimate prognosis. A three-grade system is commonly used, although some institutions employ a four-grade scheme. Grade 1 lesions (low grade) have chondrocytes with small dense nuclei, although some slightly enlarged nuclei (>8 μm) and a few multinucleated cells (most commonly binucleated) are present (1–5). The stroma is predominantly chondroid. Myxoid areas are usually sparse or absent. Distinction of grade 1 chondrosarcoma from enchondroma is often difficult.

Grade 2 chondrosarcomas (intermediate grade) have less chondroid matrix and are correspondingly more cellular (Fig 3). This increased cellularity is particularly prominent at the periphery of tumor lobules, where chondroid matrix may be completely absent and rare mitotic figures may be found (1–12). The chondrocyte nuclei in the center of the lobules are enlarged and either vesicular or hyperchromatic. Binucleated and multinucleated chondrocytes are common. Necrosis ranges from small microscopic foci to completely necrotic lobules. The stroma is frequently myxoid.

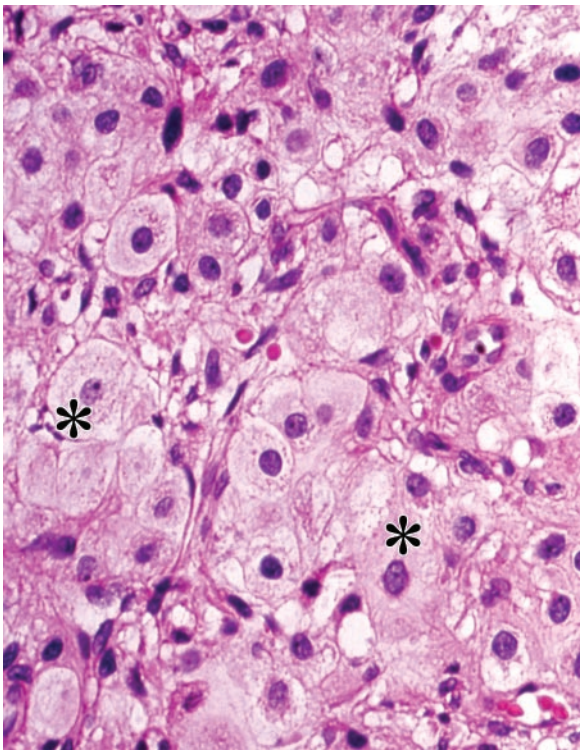

Figure 4. High-power photomicrograph (original magnification, ×250; hematoxylin-eosin stain) shows large cells with abundant clear cytoplasm (*) secondary to high glycogen content and prominent nucleoli within the nucleus, findings typical of a clear cell chondrosarcoma. Areas of typical conventional chondrosarcoma were also seen (not shown).

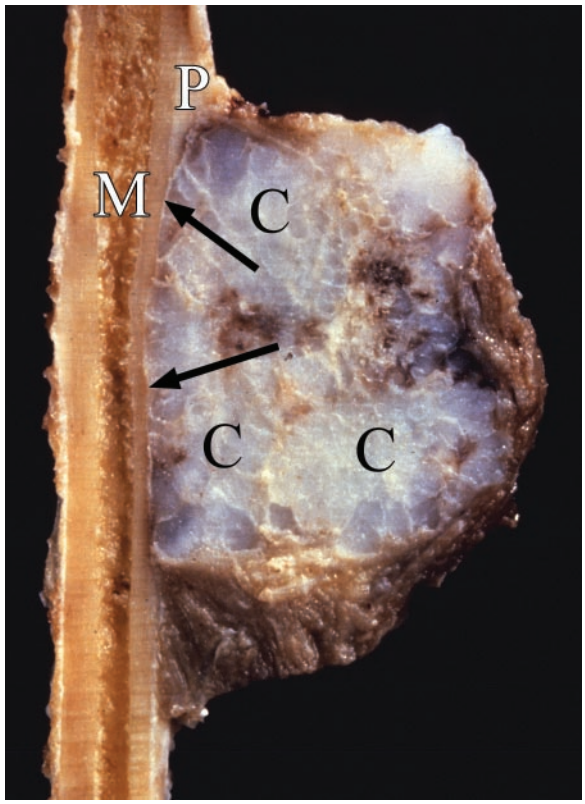

Figure 5. Photograph of an oblique longitudinally sectioned gross specimen from the left calf of a 37-year-old man with a juxtacortical chondrosarcoma shows typical lobular chondroid architecture *(C)* with extrinsic erosion of the fibula (arrows) and cortical thickening *(P)*. The marrow canal is not involved *(M)*. (For radiologic images see Fig 15.)

Grade 3 chondrosarcomas (high grade) exhibit greater cellularity and nuclear pleomorphism than grade 2 tumors (1–12). Chondroid matrix is sparse or absent, and the small amount of intercellular material present is often myxoid. The neoplastic chondrocytes are frequently arranged in cords and clumps. Individual cells commonly have stellate or markedly irregular shapes. Foci of necrosis are almost invariably seen and are frequently extensive. Nuclei are typically vesicular, are often spindle shaped, and may be five to 10 times larger than normal.

Clear Cell Chondrosarcoma

Clear cell chondrosarcoma is a rare low-grade malignant cartilaginous tumor. At histologic analysis, these lesions reveal numerous cells with abundant clear, vacuolated cytoplasm containing large amounts of glycogen (clear cell chondrocytes) that often lie between heavily calcified trabeculae of cartilage matrix and may superficially resemble bone (Fig 4). Areas of osseous metaplasia may also be prominent, bearing a striking resemblance to osteoblastoma. Unlike conventional chondrosarcoma, clear cell chondrosarcomas frequently contain large areas of hemorrhage and cyst formation. Areas of conventional chondrosarcoma are apparent in approximately 50% of clear cell chondrosarcomas (1–6).

Juxtacortical Chondrosarcoma

At gross pathologic examination, juxtacortical chondrosarcoma arises on the surface of bone and is covered by a fibrous pseudocapsule that is continuous with the underlying periosteum (Fig 5).

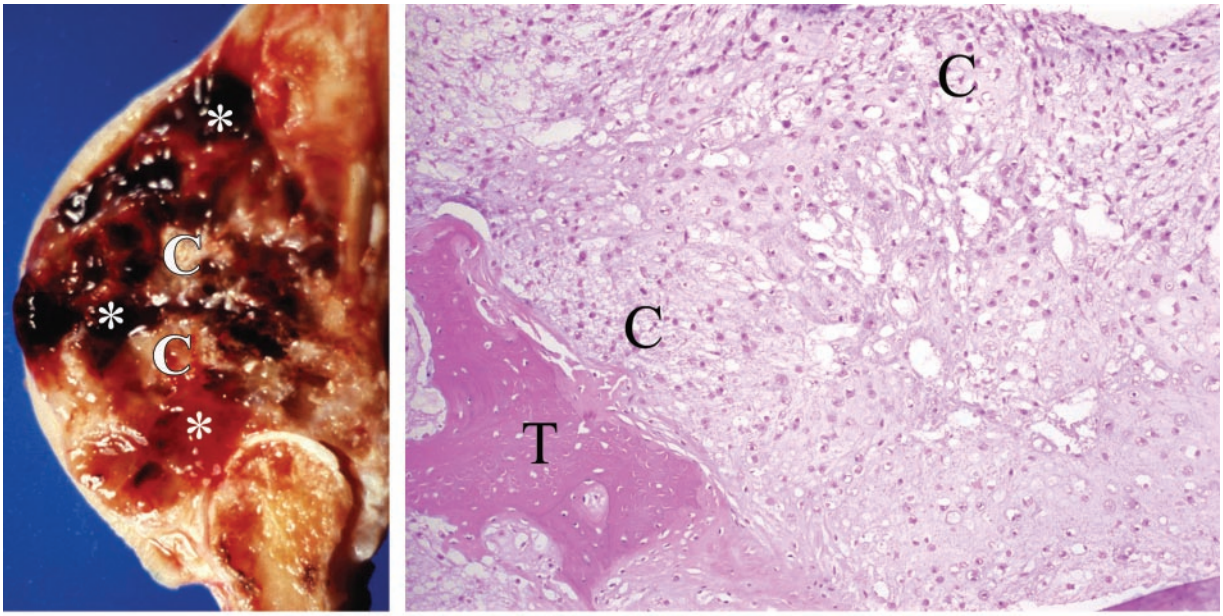

a. b.

Figure 6. Myxoid chondrosarcomas in two different patients. **(a)** Photograph of a sagittally sectioned gross specimen of an amputated finger shows gelatinous consistency of the myxoid tissue (*) and small foci of cartilage *(C)*. **(b)** Photomicrograph (original magnification, ×175; hematoxylin-eosin stain) reveals a cartilage neoplasm with prominent myxoid changes and cordlike arrangement of cells surrounding osseous trabeculae *(T)*.

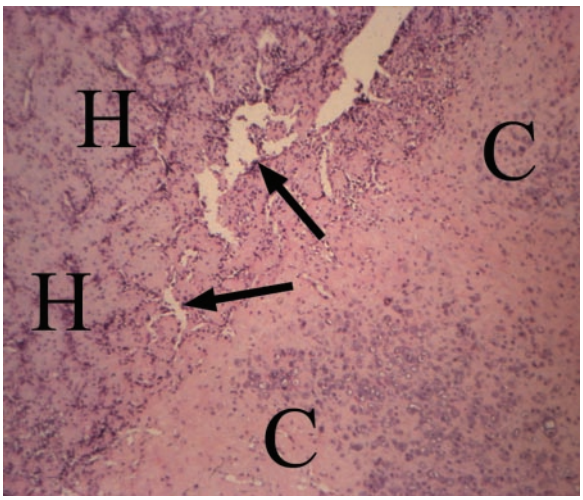

Figure 7. Photomicrograph (original magnification, ×150; hematoxylin-eosin stain) shows the typical bimorphic appearance of mesenchymal chondrosarcoma, with a malignant cartilaginous component on the right *(C)* and an abrupt transition to a more cellular vascular portion on the left *(H)* with hemangiopericytoma-like features. Arrows = vascular channels.

Cortical erosion is often present. Although medullary involvement is unusual, it has been reported. These lesions are histologically identical to conventional intramedullary chondrosarcoma with a variable degree of enchondral bone formation (1–7).

Myxoid Chondrosarcoma

Myxoid chondrosarcoma is a rare histologic variant of chondrosarcoma that occurs in both bone and soft tissue and is considered an intermediate-grade tumor. These lesions have marked high water content, related to the extensive myxoid stroma and better-differentiated areas of hyaline cartilage (Fig 6). Cellular areas are arranged in cords, resembling chordoma from which they can be difficult to differentiate (Fig 6) (4).

Mesenchymal Chondrosarcoma

These high-grade malignant cartilaginous tumors are rare and can originate in either bone or soft tissue. The characteristic histologic feature is a bimorphic pattern. Large components of the tumor are composed of small, uniform, round to spindle-shaped cells, which resemble those of Ewing sarcoma. These cellular areas also demonstrate a perivascular arrangement that results in a hemangiopericytoma-like pattern (Fig 7). However,

their characteristic focal admixed areas of limited or extensive malignant cartilaginous tissue arranged in a lobular pattern allows for accurate pathologic diagnosis (1–7).

Dedifferentiated Chondrosarcoma

This cartilaginous malignancy is characterized by conventional low-grade chondrosarcoma with abrupt transition to foci that have dedifferentiated into a higher-grade, more aggressive component. The noncartilaginous component may be either small or extensive and is most frequently malignant fibrous histiocytoma, osteosarcoma, or fibrosarcoma (Fig 8) (1–7). Rhabdomyosarcoma, leiomyosarcoma, and angiosarcoma have also been reported as the dedifferentiated component. The cartilaginous and noncartilaginous components are often adjacent, and the term *collision of two tumors* has been applied to this lesion (1).

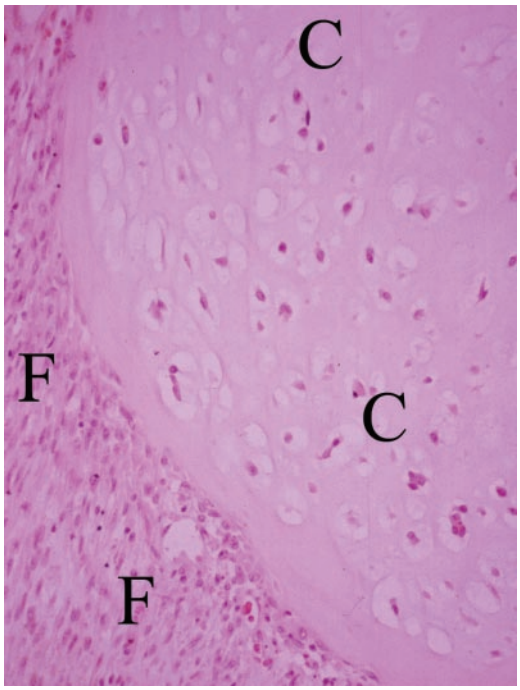

Figure 8. Photomicrograph (original magnification, ×200; hematoxylin-eosin stain) shows a "collision of two tumors" typical of a dedifferentiated chondrosarcoma, with low-grade chondrosarcoma on the right *(C)* adjacent to a high-grade fibrosarcoma component on the left *(F)* with an abrupt transition.

Clinical Characteristics and Imaging Features

Conventional Intramedullary Chondrosarcoma

Conventional intramedullary chondrosarcoma is the most common type of primary chondrosarcoma. It has also been referred to as central chondrosarcoma. Patients with conventional chondrosarcoma most commonly present in the 4th to 5th decades of life. There is a male predilection of 1.5–2 to 1. Clinical symptoms are nonspecific, with pain being the most frequent symptom, occurring in at least 95% of patients (2,13). The pain is often insidious, progressive, and worse at night and has been present for months to years before the time of presentation. A palpable soft-tissue mass or fullness has also been described in 28%–82% of patients (1–7,13). Pathologic fractures are also common at initial presentation in 3%–17% of patients with conventional chondrosarcoma (1–17).

The most common skeletal location for conventional chondrosarcoma is the long tubular bones (which are also a common site for solitary enchondroma), accounting for approximately 45% of cases (Figs 9, 10) (1–21). The femur is the single most commonly affected long bone, representing approximately 20%–35% of cases, followed in frequency by the tibia (5%) (1–21). The upper extremity is involved in 10%–20% of cases, with the proximal humerus being the most frequent site (1–21). The axial skeleton is also commonly affected, with the innominate bone (Fig 11) accounting for 25% of cases and the ribs

Figure 9. Conventional intramedullary chondrosarcoma of the humerus in a 21-year-old man with shoulder pain. **(a)** Anteroposterior shoulder radiograph shows a proximal humeral mixed lytic and sclerotic lesion with expansile remodeling. The sclerotic component represents typical chondroid ring-and-arc calcification (white arrows). Lytic focus seen inferolaterally (black arrow) demonstrates deep endosteal scalloping typical of chondrosarcoma. **(b)** Anterior bone scan shows that the lesion has radionuclide uptake greater than that in the anterior iliac spines. **(c)** Axial CT scan shows decreased attenuation of the nonmineralized component of the lesion and chondroid mineralization (arrows). **(d, e)** Axial T1-weighted fat saturation (repetition time msec/echo time msec = 600/20) MR images obtained before **(d)** and after **(e)** intravenous administration of gadolinium show signal intensity similar to that of muscle and mild peripheral and septal enhancement (arrows). **(f)** Coronal T2-weighted (3,000/57) MR image demonstrates lobular growth (large arrow) and a focus of deep endosteal scalloping with cortical penetration (small arrows) laterally. **(g)** Photograph of the coronally sectioned gross specimen shows a cartilage lesion with lobular growth (large arrow) and cortical destruction laterally (small arrows), identically correlating to imaging features.

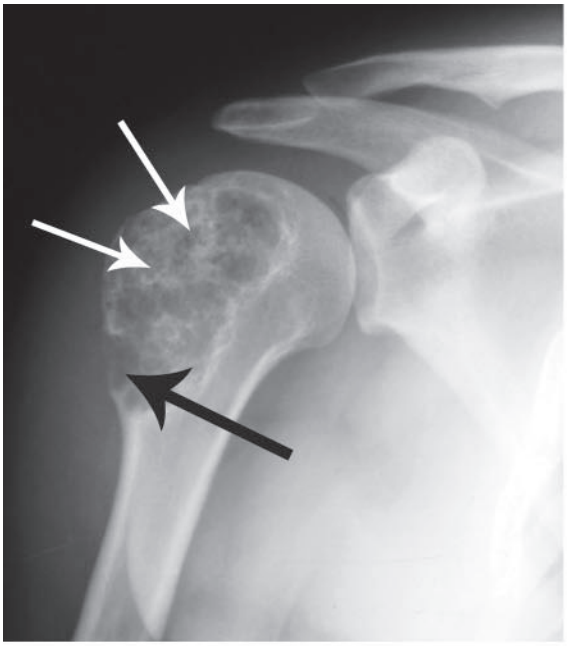

a.

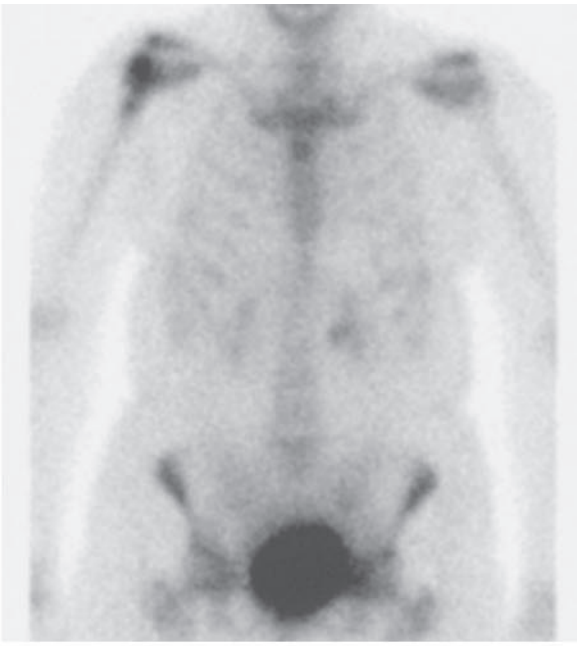

b.

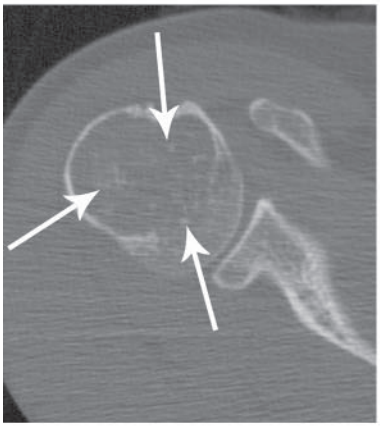

c.

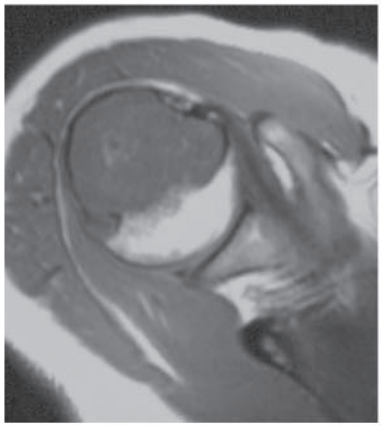

d.

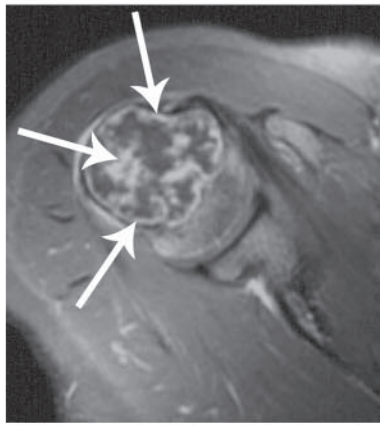

e.

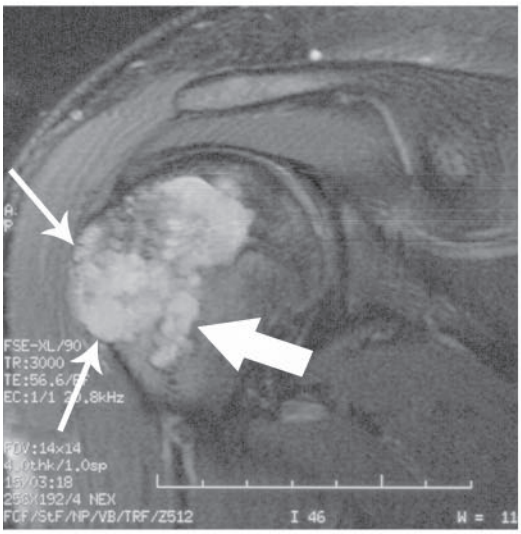
FSE-XL/90
TR:3000
FOV:14x14
256X192/4 NEX
FCF/StF/NP/VB/TRF/Z512
I 46
W = 11

f.

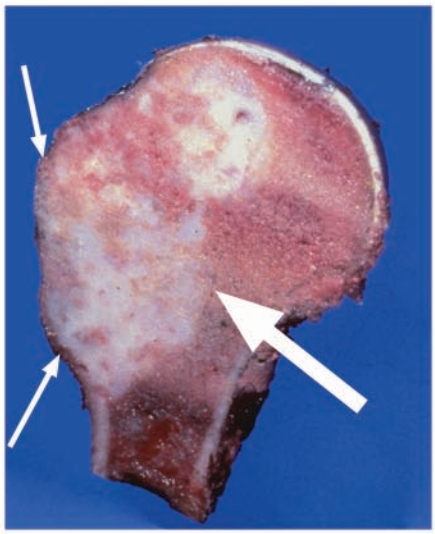

g.

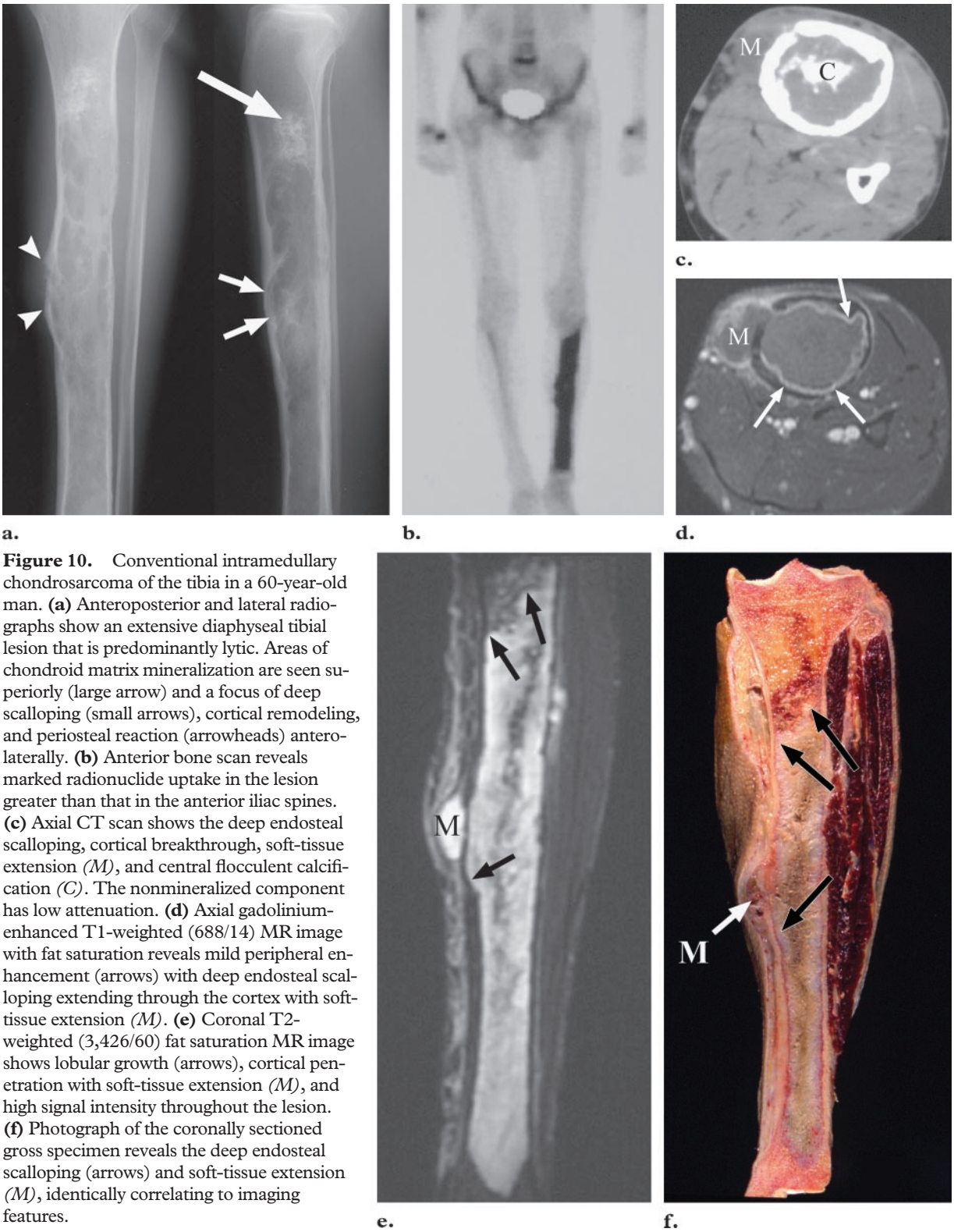

Figure 10. Conventional intramedullary chondrosarcoma of the tibia in a 60-year-old man. **(a)** Anteroposterior and lateral radiographs show an extensive diaphyseal tibial lesion that is predominantly lytic. Areas of chondroid matrix mineralization are seen superiorly (large arrow) and a focus of deep scalloping (small arrows), cortical remodeling, and periosteal reaction (arrowheads) anterolaterally. **(b)** Anterior bone scan reveals marked radionuclide uptake in the lesion greater than that in the anterior iliac spines. **(c)** Axial CT scan shows the deep endosteal scalloping, cortical breakthrough, soft-tissue extension *(M)*, and central flocculent calcification *(C)*. The nonmineralized component has low attenuation. **(d)** Axial gadolinium-enhanced T1-weighted (688/14) MR image with fat saturation reveals mild peripheral enhancement (arrows) with deep endosteal scalloping extending through the cortex with soft-tissue extension *(M)*. **(e)** Coronal T2-weighted (3,426/60) fat saturation MR image shows lobular growth (arrows), cortical penetration with soft-tissue extension *(M)*, and high signal intensity throughout the lesion. **(f)** Photograph of the coronally sectioned gross specimen reveals the deep endosteal scalloping (arrows) and soft-tissue extension *(M)*, identically correlating to imaging features.

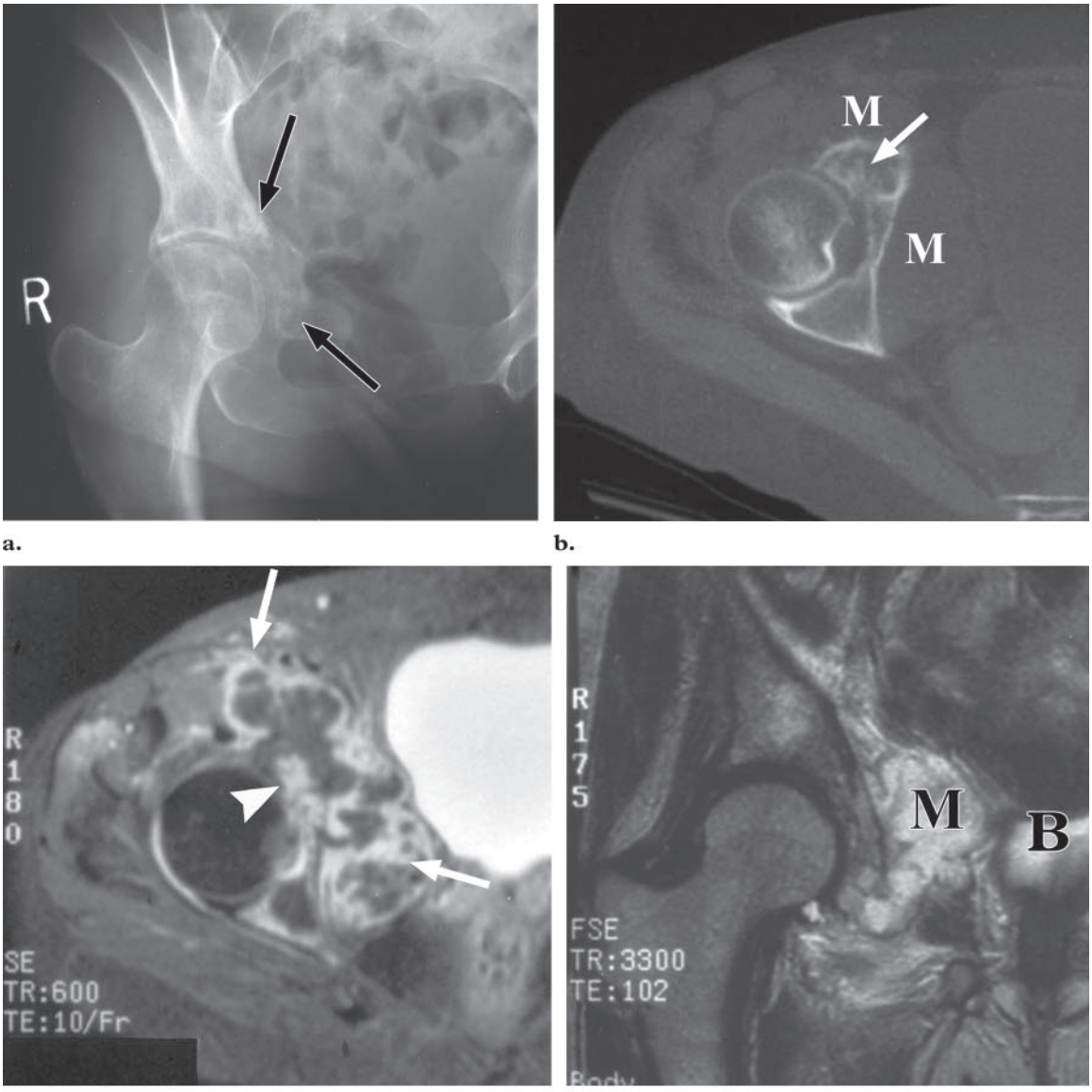

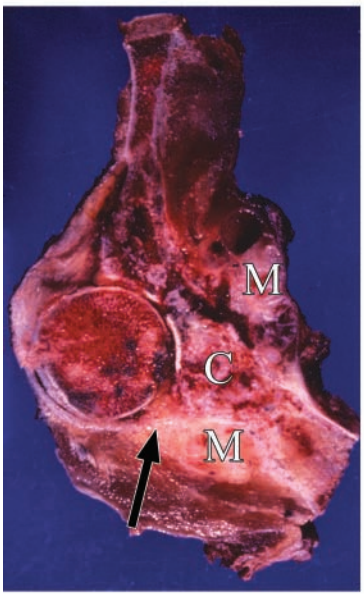

Figure 11. Conventional intramedullary chondrosarcoma of the acetabulum in a 52-year-old woman with a 2-year history of right hip and leg pain. **(a)** Anteroposterior hip radiograph shows subtle sclerosis caused by chondroid matrix mineralization and bone destruction of the ilium and iliopectoneal line cortex lesion center at the previous site of the triradiate cartilage (arrows). **(b)** Axial CT scan reveals an extensive low-attenuation soft-tissue mass *(M)* about the hip and faint intraosseous matrix mineralization (arrow). **(c)** Axial gadolinium-enhanced T1-weighted (666/10) MR image with fat saturation demonstrates peripheral and septal enhancement of both the soft-tissue and intraosseous components of the tumor (arrows) with hip joint invasion (arrowhead). **(d)** Coronal T2-weighted (3,300/102) MR image demonstrates soft-tissue extension *(M)* and high signal intensity similar to that of the bladder *(B)*. **(e)** Photograph of the sagittally sectioned gross specimen demonstrates extensive marrow involvement *(C)*, the soft-tissue mass *(M)*, and joint invasion inferiorly (arrow).

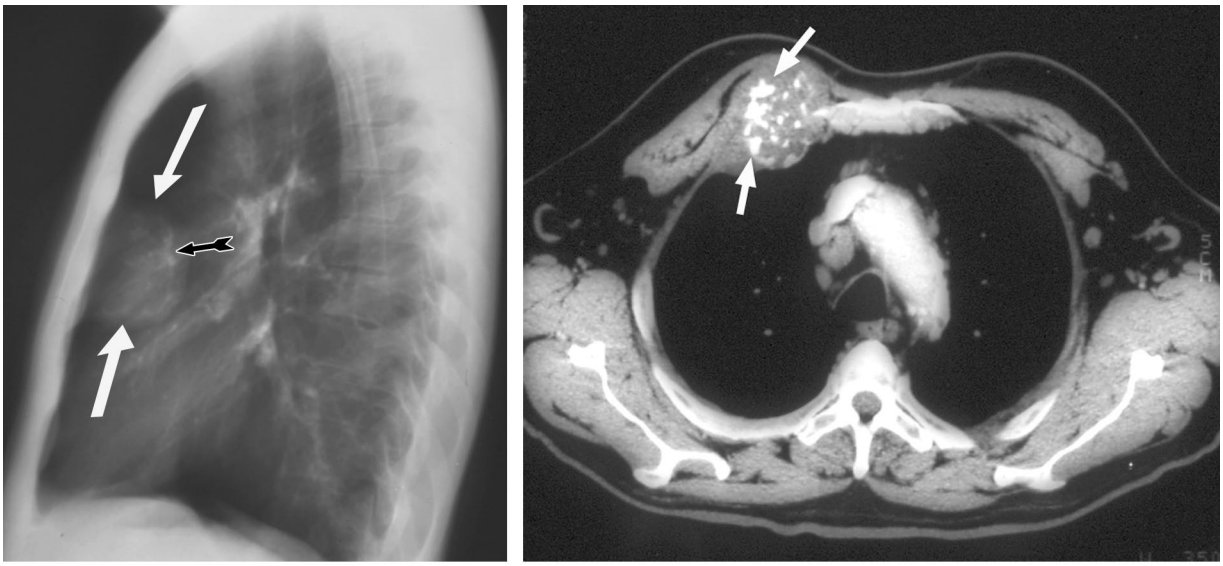

a. b.

Figure 12. Conventional chondrosarcoma of the rib in a 70-year-old man who presented with a painless anterior chest wall mass. **(a)** Lateral chest radiograph shows a mass (white arrows) overlying an anterior rib. Faint calcific opacity is seen (black arrow). **(b)** Axial CT scan demonstrates prominent chondroid matrix mineralization (arrows) to much better advantage and involvement of the costosternal junction. **(c)** Photograph of the axially sectioned gross specimen reveals the lesion clearly arising from the anterior rib and costal junction *(R,* arrows) and the lobular growth architecture *(C)* typical of hyaline cartilage neoplasms.

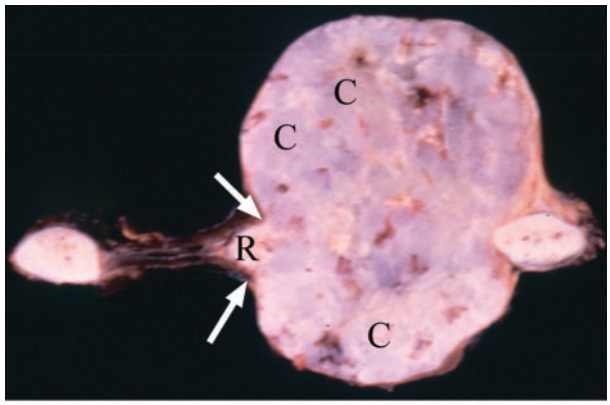

c.

8% (Fig 12) (1–3). Other less frequently involved sites are the spine (7% of cases), scapula (5%), and sternum (2%) (1–10). Chondrosarcoma can involve any bone, and rarely affected locations include the craniofacial region (Fig 13), neck (arising from the hyoid as well as laryngeal and tracheal cartilage), forearm, clavicle, sesamoids (including the patella), and the short tubular bones of the hands and feet (1%–4% of all cases) (1–3). Fibular origin has also been reported as rare, but this has not been our experience (7% of long bone lesions) (13). Long tubular bone lesions most commonly involve the metaphysis (49% of cases), followed by the diaphysis (36%) (13). Conventional chondrosarcomas centered in the epiphysis are unusual, accounting for only 16% of cases (13). In contrast, solitary epiphyseal enchondromas are rare. Chondrosarcomas involving the humerus and fibula are almost invariably proximal. Similarly, lesions in the femur and tibia are more common proximally.

Radiographs of conventional chondrosarcoma typically reveal a mixed lytic and sclerotic appearance (Figs 9–12). The sclerotic areas represent chondroid matrix mineralization and are seen in 60%–78% of lesions (Figs 9–12) (1–5,13). The characteristic appearance of mineralized chondroid matrix is a ring-and-arc pattern of calcification (13,22–31). This pattern may coalesce to form a more radiopaque flocculent pattern of calcification. This characteristic chondroid calcification usually allows confident radiologic diagnosis of a cartilaginous lesion and is often the most dominant feature. This radiographic appearance represents the pathologic characteristic of enchondral ossification about the margins of the cartilaginous lobules. Higher-grade chondrosarcomas often contain relatively less extensive areas of matrix mineralization. The radiolucent component usually reveals geographic bone lysis and is multilobulated, directly corresponding to the growth pattern of this hyaline cartilage lesion (Figs 9, 10). More aggressive patterns of bone lysis (moth-eaten and permeative) may be seen with higher-grade conventional chondrosarcomas (grade 3), but they are much more frequently associated with mesenchymal, myxoid, and

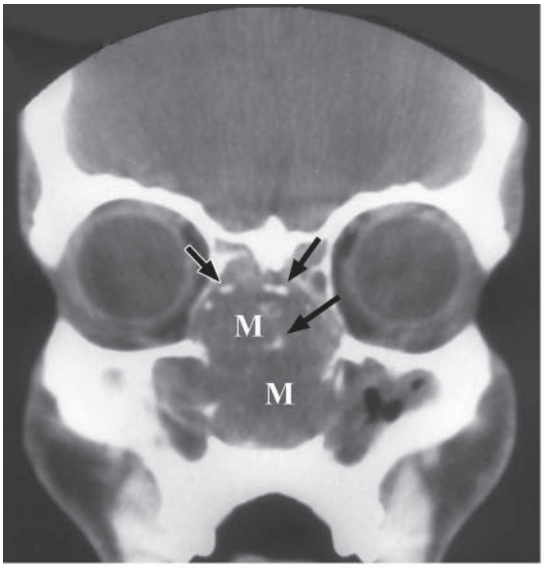

a.

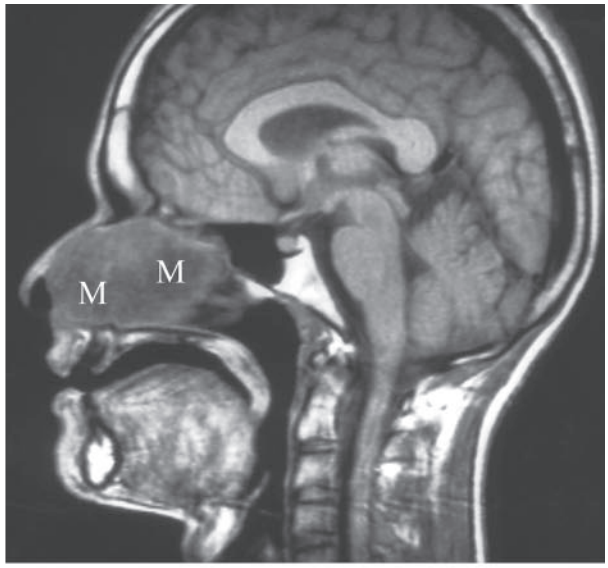

b.

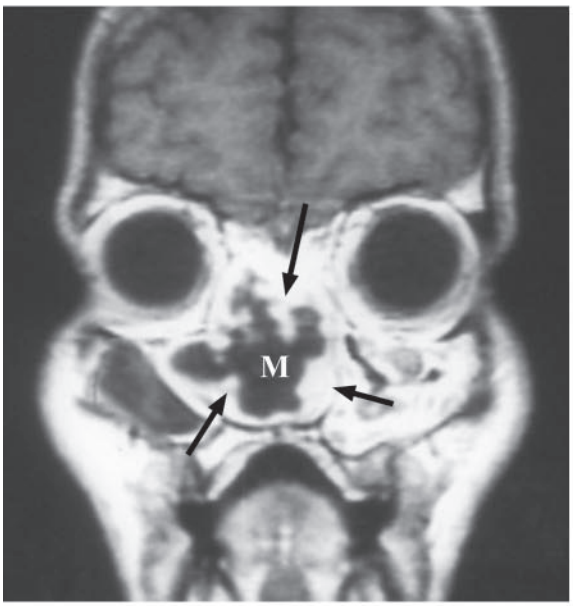

c.

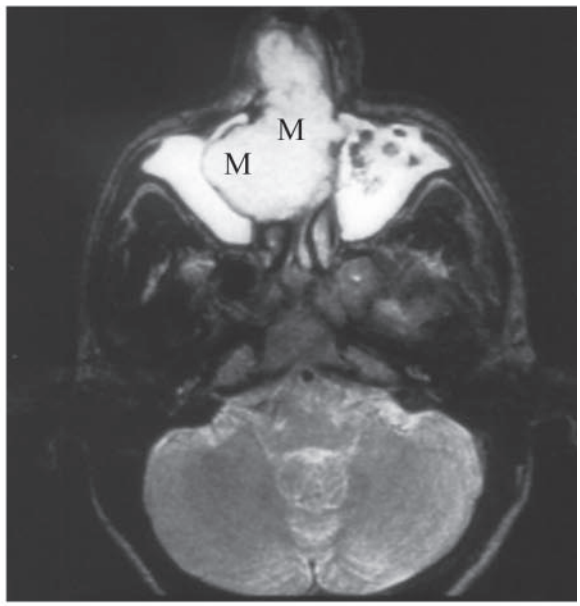

d.

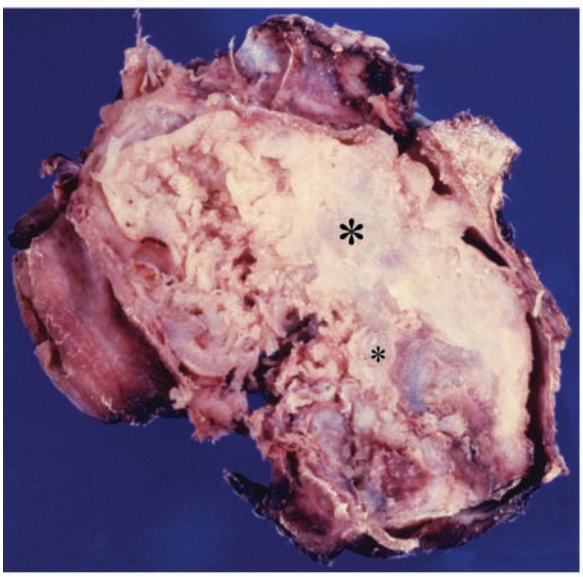

e.

Figure 13. Craniofacial conventional chondrosarcoma in a 26-year-old man with nasal symptoms. **(a)** Coronal CT reformatted image reveals a low-attenuation mass *(M)* replacing nasal bones and displacing the nasal septum with small subtle chondroid matrix mineralization (arrows). **(b, c)** Sagittal T1-weighted (570/15) MR image obtained without **(b)** and coronal T1-weighted MR image (570/15) obtained with **(c)** gadolinium show the low-signal-intensity mass *(M)* with mild peripheral and septal enhancement (arrows) replacing the area of the cribriform plate in the anterior cranial skull base and extending into the nasal region. Severe sinus disease is seen. **(d)** Axial T2-weighted fat saturation (2,200/80) MR image shows that the mass *(M)* erodes the medial wall of the right maxillary sinus and left maxillary sinus with marked high signal intensity similar to that of mucosal thickening and fluid in both sinuses. Matrix mineralization cannot be seen. **(e)** Photograph of the gross specimen show portions of the cribriform plate superiorly, maxillary sinus, and lobules of cartilage growth (*).

dedifferentiated cell types. Continued growth leads to lobulated endosteal scalloping that eventually produces cortical penetration (57% of long bone lesions on radiographs) and a soft-tissue component (46% of long bone lesions on radiographs) (Figs 9–11) (13). In our experience, the depth of endosteal scalloping at its most prominent focus is the best distinguishing feature between long bone enchondroma and chondrosarcoma (13,22). Endosteal scalloping greater than two-thirds the normal thickness of the long bone cortex is strong evidence of chondrosarcoma (75% of cases on radiographs) versus enchondroma (9% of cases on radiographs) (Figs 9, 10) (13). Extensive, longitudinal, endosteal scalloping in long bone lesions (along greater than two-thirds of lesion length) is also more suggestive of conventional chondrosarcoma than enchondroma, although it is not as distinctive a feature as the depth of scalloping.

Endosteal scalloping reflects lobular lesion growth and an attempt by the intramedullary malignancy to extend to a second compartment. However, because of the relatively slow growth of the lesion, the cortex responds to maintain the tumor in the medullary canal. This attempt to maintain a margin about the chondrosarcoma frequently leads to cortical remodeling, cortical thickening, and periosteal reaction, all of which are uncommonly associated with enchondroma. These findings are most likely to be seen in long bone lesions.

Bone scintigraphy usually reflects the increased physiologic activity of conventional intramedullary chondrosarcoma (13,21,32,33). The majority (82%) of long bone chondrosarcomas reveal marked increased radionuclide uptake compared with that in the anterior iliac crest, in contrast to long bone enchondromas, which show increased radiotracer activity in only 21% of cases (Figs 9, 10) (13). In addition, a heterogeneous pattern of radionuclide uptake is also more common in conventional intramedullary chondrosarcoma (63% of long bone chondrosarcomas versus 30% of enchondromas) (13). Technetium-99m–labeled dimercapto succinic acid (DMSA) radionuclide activity was seen in all cases of chondrosarcoma in a series of cases reported by Kobayashi and colleagues (33). In the future, positron emission tomography may be employed to help distinguish chondrosarcoma from enchondroma (34–36).

CT allows optimal detection and characterization of matrix mineralization, particularly when it is subtle or the lesion is in a complex area of anatomy. Areas of matrix mineralization are demonstrated by CT in 94% of long bone chondrosarcomas (Figs 9–12) (13). Neither the extent nor the presence of matrix mineralization identified on CT scans helps distinguish between long bone enchondroma and chondrosarcoma. The high sensitivity of CT for depiction of matrix mineralization (as compared with radiography) typically shows the matrix mineralization to be throughout the lesion.

Evaluation of endosteal scalloping depth is also aided by the three-dimensional imaging provided by CT compared with two-dimensional radiography (13,22–31,37–40). Long bone chondrosarcomas have focal areas of greater than two-thirds scalloping of the normal cortical thickness in 90% of cases, as opposed to enchondromas, which demonstrate this finding in only 10% of cases on CT scans (Figs 9, 10) (13). The longitudinal extent of endosteal scalloping on CT scans is usually throughout the lesion length in long bone chondrosarcomas (79%), as opposed to a shorter extent with enchondromas (13,21). Lobulated endosteal scalloping causing cortical destruction is common in long bone conventional chondrosarcomas on CT scans (88% of long bone lesions) but rare in enchondroma (8%) (13). Cortical response, including cortical thickening and periosteal reaction, to the chondrosarcoma in an attempt to confine the process to the medullary canal is equally well demonstrated with CT and radiography (30–40).

As expected, identification of soft-tissue extension on CT scans is more frequent than on radiographs. Soft-tissue involvement, which occurs in 59% of long bone chondrosarcomas on CT scans, essentially excludes the possible diagnosis of enchondroma (Figs 9–12) (13). We believe the size of the soft-tissue component may well parallel the histologic characteristics of the lesion, with higher-grade lesions being larger size. The soft-tissue component frequently reveals typical punctate or ring-and-arc matrix mineralization and a lobular growth pattern. The nonmineralized components, both intraosseous and extraosseous,

typically have low attenuation on CT scans, reflecting the high water content of hyaline cartilage (Figs 10c, 13a). CT performed after intravenous administration of contrast material demonstrates mild peripheral rim and septal enhancement. Higher-grade lesions may show higher CT attenuation, similar to that of muscle, and more prominent diffuse or nodular contrast enhancement, caused by increased cellularity and resultant reduced water content.

MR imaging provides the best method for depicting the extent of marrow involvement by conventional intramedullary chondrosarcoma (13,41–48). On T1-weighted MR images, marrow replacement appears as low to intermediate signal intensity. Entrapped areas of preexisting yellow marrow may be seen as small speckled punctate regions of high signal intensity on T1-weighted MR images in long bone intramedullary chondrosarcomas (35% of lesions) but are much less common than in enchondromas (65%) (13). This difference reflects the more aggressive growth of malignant cartilaginous neoplasms. The lobular architecture typical of all hyaline cartilage neoplasms is commonly seen best at the lesion margin (78% of long bone chondrosarcomas on MR images) (Figs 9, 10) (13). The nonmineralized components of chondrosarcoma have high signal intensity on T2-weighted MR images, again a reflection of the high water content of hyaline cartilage (Figs 9–11). The cartilaginous lobules may be surrounded by low-signal-intensity septa. Areas of matrix mineralization are common in intramedullary chondrosarcoma (79% of long bone lesions on MR images) and have low signal intensity with all MR pulse sequences (13). This feature often creates marked heterogeneity on T2-weighted MR images. However, the detection and particularly the characterization of matrix mineralization is superiorly achieved with radiography and CT. Areas of low signal intensity on T2-weighted MR images, although corresponding to matrix mineralization, are nonspecific and have numerous other potential causes, including fibrous tissue with high collagen content and other types of calcification.

Both the depth and extent of endosteal scalloping are well depicted by MR imaging, particularly with proton-density–weighted sequences. CT and MR imaging are superior to radiography in this evaluation because the entire cortical circumference is seen with these cross-sectional imaging modalities, as opposed to the tangential view of a small part of the cortex seen with radiography (13,21,26). The depth of endosteal scalloping seen on MR images is again the more discriminating factor in distinguishing long bone chondrosarcoma from enchondroma. Endosteal scalloping of more than two-thirds of the normal cortical thickness is seen in 85% of long bone intramedullary chondrosarcomas versus only 6% of enchondromas (Figs 9, 10) (13). The extent of endosteal scalloping on MR images is more prominent in long bone intramedullary chondrosarcoma than enchondroma. Endosteal scalloping causing cortical destruction is commonly seen on MR images of long bone intramedullary chondrosarcoma (73% of cases) (Figs 9, 10) (13). The response of bone in an attempt to contain the intramedullary chondrosarcoma in the marrow cavity, as evidenced by cortical remodeling, cortical thickening, and periosteal reaction, is also seen on MR images, although not as clearly as on radiographs or CT scans. Peritumoral edema, which is best seen with water-sensitive MR imaging sequences, has also been reported to suggest conventional intramedullary chondrosarcoma rather than enchondroma (46).

As with CT, MR imaging demonstration of soft-tissue extension with mass formation essentially excludes the diagnosis of enchondroma (41–48). MR imaging, primarily because of its superior contrast resolution, is the best radiologic modality with which to identify soft-tissue extension, which is seen in 76% of long bone conventional intramedullary chondrosarcomas (Figs 10, 11) (13). The intrinsic characteristics of the soft-tissue extension on MR images are identical to those of the intraosseous component.

The contrast enhancement pattern of conventional intramedullary chondrosarcoma is typically mild in degree and peripheral and septal in pattern (Figs 9–11). This pattern was initially described by Aoki and colleagues (41). Some researchers, including De Beuckeleer et al (42,43) and Geirnaerdt et al (22,44,45), believe that this pattern of enhancement allows differentiation of intramedullary chondrosarcoma from enchondroma (which has peripheral enhancement only). Similarly, dynamic subtraction MR imaging

with early enhancement has been proposed as a method to distinguish low-grade chondrosarcoma from enchondroma (42–45). However, in our experience, these different patterns of enhancement do not allow reliable distinction between low-grade intramedullary chondrosarcoma and enchondroma (Fig 10d) (13,21). This position is analogous to that of the pathologists, who do not use differences in vascularity as a significant criterion for distinguishing between these lesions (49,50). In our experience, higher-grade lesions appear with larger soft-tissue masses, with somewhat lower signal intensity on T2-weighted images and more prominent diffuse or nodular contrast enhancement on MR images, similar to their appearance on CT scans.

The following subsections describe the characteristics of conventional intramedullary chondrosarcoma in specific anatomic locations.

Pelvis.—In contradistinction to the long bones, in which both enchondroma and chondrosarcoma are frequent, the pelvis is a common site for chondrosarcoma and an extraordinarily rare one for solitary enchondroma (not associated with enchondromatosis) (1–5). Pelvic chondrosarcomas most frequently involve the ilium, with a particular predilection for the area around the previous region of the triradiate cartilage (Fig 11). Pelvic chondrosarcomas are often large lesions at initial evaluation owing to the delay in onset of clinical symptoms (10). Paradoxically, although lesions are large, radiographs may be only subtly abnormal because of the complex anatomy of the pelvis (Fig 11) (10,21). CT or MR imaging invariably demonstrates aggressive features with cortical destruction and a large soft-tissue mass (Fig 11). Areas of matrix mineralization are frequently detected only on CT scans, again because of pelvic anatomic complexity. Hip joint invasion and iliac adenopathy may also occur.

Ribs and Sternum.—The vast majority of solitary lesions (not associated with enchondromatosis) with chondroid matrix mineralization in the ribs and sternum are chondrosarcomas, and solitary enchondromas are extremely rare (51–57), similar to the lesions found in the pelvis. Occasionally, chondrosarcomas in the ribs and sternum may be discovered incidentally at chest radiography. Patients are often somewhat younger than those with conventional chondrosarcomas in other sites (51). Rib lesions usually involve the anterior rib at the costochondral junction and show osseous expansile remodeling with a ring-and-arc pattern of calcification and soft-tissue extension on both radiographs and CT (Fig 12) (51–57). Sternal lesions are more problematic to detect on radiographs owing to the difficulty in imaging the sternum with radiography. CT of sternal chondrosarcomas, similar to that of rib lesions, reveals typical chondroid mineralization and soft-tissue extension (56).

Hands and Feet.—In contradistinction to the pelvis, ribs, and sternum, the hands and feet are rare sites for intramedullary chondrosarcomas, whereas enchondromas are extraordinarily common in these sites (58,59). Enchondromas of the short tubular bones of the hands and feet frequently cause deep endosteal scalloping. Thus, this criterion cannot be used to distinguish enchondroma from chondrosarcoma in the hands or feet as it can in the long bones. The differentiation between benign and malignant cartilage lesions in short tubular bones is very difficult radiologically, unless there is clear evidence of extension through the cortex and an associated soft-tissue mass (58–60).

Vertebral Column.—Chondrosarcoma represents the second most common nonlymphoproliferative primary malignant tumor in the vertebrae of adults, with the most frequent being chordoma (61–65). Solitary enchondromas of the spine are very rare. Neurologic symptoms are apparent in 45% of patients, and men are affected two to four times more frequently than women (61–65). The thoracic spine is most frequently affected. In our experience, the sacrum is a rare site for primary chondrosarcoma. Lesions more commonly originate in the posterior elements of the spine (40% of cases) as opposed to the vertebral bodies (15%) (64). In 45% of cases, both vertebral body and posterior elements are involved at presentation

(61–65). Radiographs reveal bone destruction with chondroid matrix mineralization in 70% of cases, although, as is typical of lesions in complex anatomic areas, this manifestation is more easily detected with CT (61–65). Vertebral chondrosarcomas commonly have soft-tissue components, and because these lesions are usually low grade, high water content is seen in the nonmineralized areas on CT or MR images. These modalities demonstrate the relationship of the lesion to the spinal canal and its contents as well as surrounding structures. Extension through the intervertebral disc has been reported in approximately 35% of cases, and the adjacent ribs may also be involved (64).

Craniofacial Region.—Craniofacial chondrosarcomas account for 2% of all chondrosarcomas and have a predilection for the skull base (probably related to the fact that this portion of the calvaria is preformed in cartilage) (Fig 13) (66,67). Although only 6% of skull base tumors are chondrosarcomas, benign chondroid tumors of the skull base are rare (68). Therefore, solitary intramedullary cartilaginous tumors at this site, similar to lesions in the pelvis, ribs, sternum, and spine, should always be regarded as malignant. Facial lesions most commonly involve the maxilla and may affect younger patients. Skull base chondrosarcomas involving the clivus may be confused with chordomas (66,67). Chordoma is a more common tumor in the skull base than chondrosarcoma. Differentiation between these two skull base neoplasms is very important because chondrosarcoma has a much better prognosis (66,67). The major clinical distinctions between chordomas and chondrosarcomas of the skull base are patient age and rate of growth. Chordomas tend to occur, on average, in patients a decade older than do chondrosarcomas and grow much more rapidly (68,69). Unfortunately, these distinctions are not true for mesenchymal chondrosarcomas involving the craniofacial region that also grow rapidly. Skull base chondrosarcomas have also been confused with meningiomas and metastases, the latter usually having a much worse prognosis than chondrosarcomas (66–71). Skull base chondrosarcomas are often very large at presentation, compressing the brain stem and invading adjacent areas such as the cavernous sinus (70,71), and are usually low-grade lesions histologically.

In a series of 17 cases, the age range of patients with skull base chondrosarcomas was 14–65 years, with a mean age of 36 years (69). The majority of patients (59%) were between 30 and 44 years of age, and the male-to-female ratio was 2.4:1 (66–70). The majority of these tumors (71%) were located in the petrous apex (69). The second most frequent site was the clivus (12% of cases) (69). The maxilla, orbit, and foramen magnum were each the site of the tumor in one patient (6%) (69).

CT and MR imaging reveal bone destruction and large associated soft-tissue masses that, in our experience, usually contain punctate areas of chondroid mineralization (seen with CT) (Fig 13). Nonmineralized areas show typical high water content on CT and MR images (as previously discussed) (Fig 13). As is true for chondrosarcomas in other regions, MR imaging is optimal for depicting areas of tumor involvement but not subtle matrix mineralization.

In our experience, both CT and MR imaging performed after administration of contrast material show mild peripheral and septal enhancement typical of chondroid lesions, which have been described as variegated or having a "pepper-and-salt" appearance. This appearance corresponds to a lack of perfusion at MR angiography, a feature that helps distinguish these lesions from other more vascular skull base tumors, such as metastases and meningiomas. Similarly, skull base chondrosarcomas appear relatively avascular at digital subtraction angiography (66).

Clear Cell Chondrosarcoma

Clear cell chondrosarcoma is a rare bone neoplasm that constitutes approximately 1%–2% of all chondrosarcomas and 0.2% of all primary bone tumors that lead to biopsy (1–5). Unni et al first described this lesion in 1976 (72) in a report of 16 cases. Patients are most commonly affected in the 3rd to 5th decade of life. Men are affected

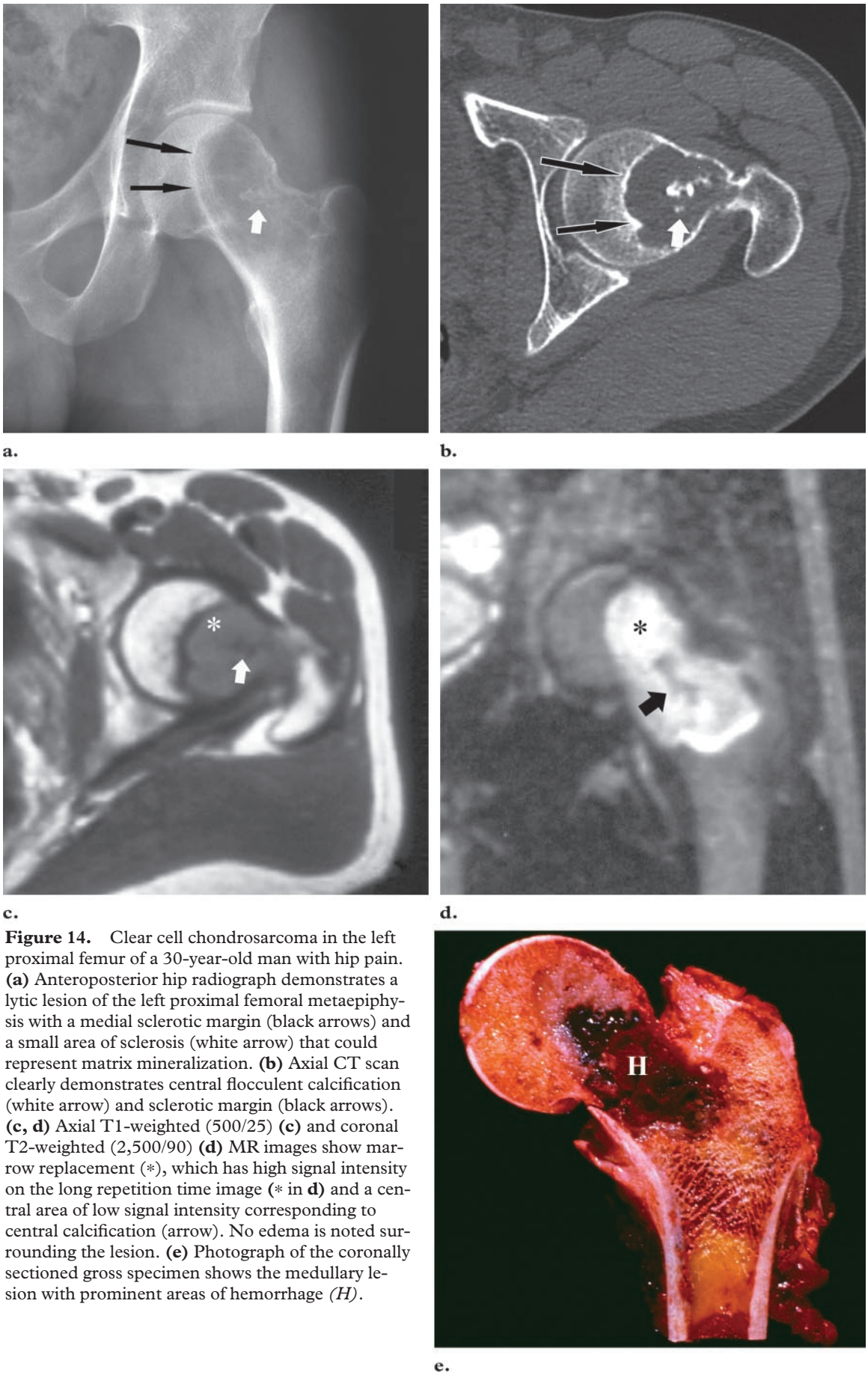

Figure 14. Clear cell chondrosarcoma in the left proximal femur of a 30-year-old man with hip pain. **(a)** Anteroposterior hip radiograph demonstrates a lytic lesion of the left proximal femoral metaepiphysis with a medial sclerotic margin (black arrows) and a small area of sclerosis (white arrow) that could represent matrix mineralization. **(b)** Axial CT scan clearly demonstrates central flocculent calcification (white arrow) and sclerotic margin (black arrows). **(c, d)** Axial T1-weighted (500/25) **(c)** and coronal T2-weighted (2,500/90) **(d)** MR images show marrow replacement (*), which has high signal intensity on the long repetition time image (* in **d)** and a central area of low signal intensity corresponding to central calcification (arrow). No edema is noted surrounding the lesion. **(e)** Photograph of the coronally sectioned gross specimen shows the medullary lesion with prominent areas of hemorrhage *(H)*.

twice as often as women (1–5). The lesion is slow growing and less aggressive than higher-grade conventional chondrosarcoma, with resultant improvement in prognosis. Symptoms include localized pain and decreased range of motion of the adjacent joint. Pathologic fracture is the cause for initial clinical presentation in approximately 25% of cases (1–4,72). Clear cell chondrosarcoma affects the long tubular bones in 85%–90% of cases, with a particular predilection for the proximal femur (Fig 14) (55%–60%) and proximal humerus (15%–20%) (1–7). Involvement about the knee is seen in 10%–15% of cases (1–5). There is also a marked predilection for epiphyseal involvement, although metaphyseal extension is common (Fig 14). Flat bones are affected in up to 10% of cases (1–5). Polyostotic involvement has been reported, although this manifestation may represent metastatic disease (72).

Radiographs reveal a predominantly lytic lesion with either a narrow or wide zone of transition. Matrix mineralization is not as frequently apparent in clear cell chondrosarcoma (approximately 30% of cases), as compared with conventional chondrosarcoma (1–5,72–76). In up to 20% of cases, a peripheral rind of sclerosis is apparent, a finding that simulates a benign lesion (Fig 14) (1–6). In approximately 30% of cases, mild expansile remodeling of bone may be apparent, particularly in larger lesions, although soft-tissue extension is unusual (<10% of cases) (1–5). Compared with radiography, CT (as it does for other chondroid lesions) can better demonstrate matrix mineralization, cortical destruction, or soft-tissue extension (Fig 14). The nonmineralized areas typically have low attenuation on CT scans.

MR imaging of clear cell chondrosarcoma typically shows homogeneous intermediate signal intensity with T1-weighted sequences and heterogeneous high signal intensity with T2-weighted sequences (Fig 14) (74–76). One author has reported heterogeneous low to intermediate signal intensity on T2-weighted MR images, findings that may correspond to lesions with marked mineralization or osseous metaplasia as can be seen histologically (75). These lesions show heterogeneous enhancement when intravenous gadolinium is used.

Because of the epiphyseal location, clear cell chondrosarcoma can be difficult to distinguish from chondroblastoma, particularly with smaller lesions. Patients with clear cell chondrosarcoma are usually 1 to 2 decades older than those with chondroblastoma (75,77). Imaging features that suggest clear cell chondrosarcoma as opposed to chondroblastoma include a large lesion, lack of surrounding edema, and high signal intensity on T2-weighted MR images. In contrast, the vast majority of chondroblastomas have low to intermediate signal intensity with all MR pulse sequences (in the solid noncystic components) in our experience (75,77).

Juxtacortical Chondrosarcoma

Lichtenstein (78) provided the initial description of juxtacortical chondrosarcoma in 1955. The first detailed description of this lesion was a report of seven cases by Schajowicz in 1977 (79). These are rare lesions, accounting for 4% of all chondrosarcomas (1–5). Juxtacortical chondrosarcoma, which arises on the surface of bone, has also been referred to as periosteal and parosteal chondrosarcoma.

Juxtacortical chondrosarcoma most frequently affects adults in the 3rd to 4th decade of life and has a mild male predilection. Clinical signs and symptoms are nonspecific and most commonly are a palpable and painless, slowly growing mass. Lesions are most frequently seen on the surface of long bones, particularly the posterior distal femoral metaphysis or diaphysis. The innominate bone is also often involved, and lesions at this site can be associated with urinary tract symptoms.

Radiographs demonstrate a round to oval lobulated soft-tissue mass on the surface of bone (Fig 15). Typical chondroid matrix mineralization is usually present. In addition, metaplastic ossification is often apparent to a variable extent

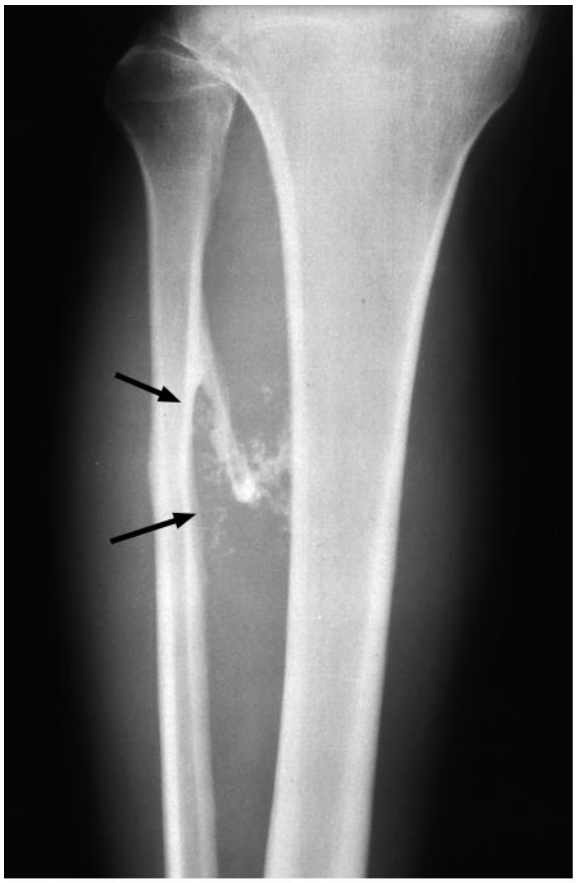

a.

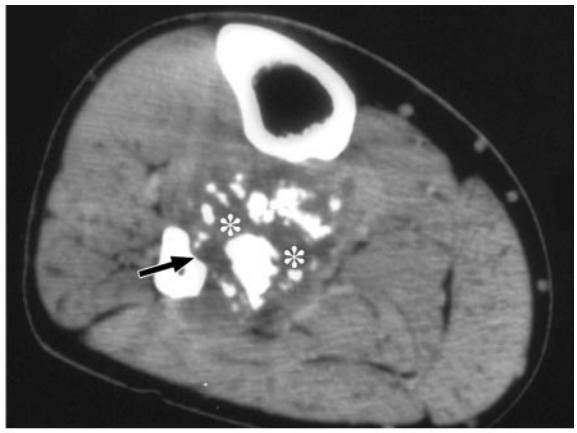

b.

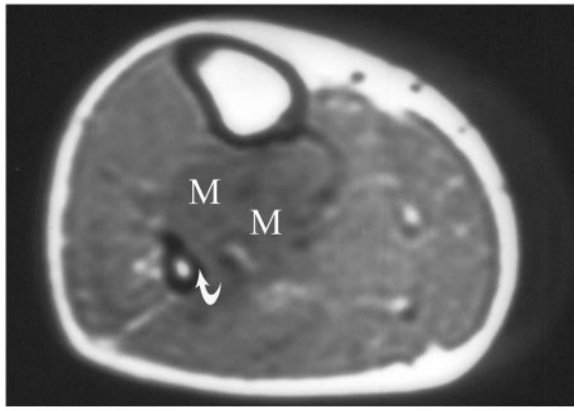

c.

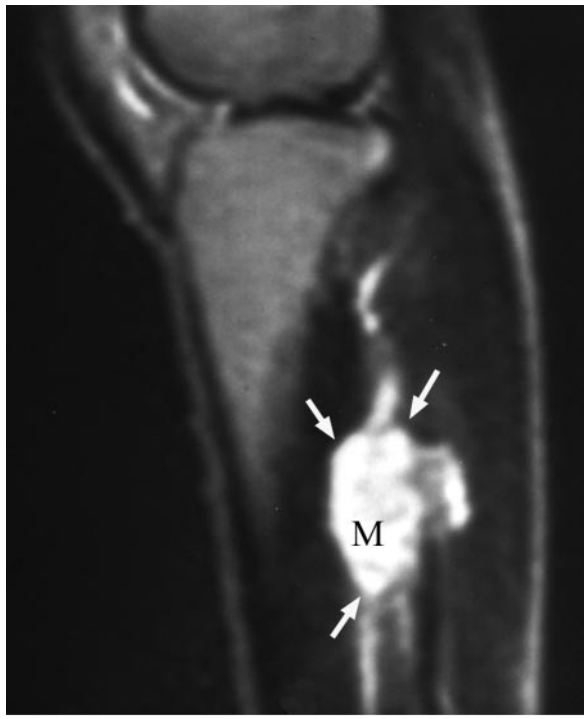

d.

Figure 15. Juxtacortical chondrosarcoma of the fibula in a 37-year-old man who had a painful lump in his right lower leg for 1 year. **(a)** Anteroposterior radiograph shows a soft-tissue mass with osteoid and chondroid mineralization between the tibia and fibula at the proximal diaphysis and extrinsic erosion of the fibula (arrows). **(b)** Axial CT scan reveals a mass with prominent mineralized matrix, low attenuation in the nonmineralized portion of the lesion (*) typical of cartilaginous neoplasms, and extrinsic erosion of the fibula (arrow) but no involvement of the marrow. **(c)** Axial T1-weighted (600/12) MR image demonstrates the low-signal-intensity juxtacortical lesion *(M)* adjacent to the proximal fibular diaphysis with extrinsic erosion (arrow) but no marrow involvement. **(d)** Sagittal T2-weighted (2,000/80) MR image demonstrates marked high signal intensity in the mass *(M)* and lobular margins (arrows) (see Fig 5).

and may be a prominent feature (Fig 15). The underlying cortex is frequently thickened with associated saucerization and Codman triangles at the lesion margins (1–3,78–84). Additional periosteal reaction, particularly perpendicular ("hair-on-end"), is absent, as is an ossific stalk of attachment to the cortex (1–3,78–84). As is true for other chondrosarcomas, matrix mineralization is better appreciated on CT scans. Nonmineralized areas show less attenuation than muscle on CT scans (Fig 15b). On MR images, the lesion shows low heterogeneous signal intensity with T1-weighted pulse sequences and heterogeneous high signal intensity with T2-weighted pulse sequences (Fig 15). Use of intravenously administered contrast material with CT or MR imaging often reveals peripheral and septal enhancement. The medullary canal is typically not involved, although extension has been observed on MR images.

Radiologic differential diagnosis primarily includes juxtacortical chondroma, parosteal osteosarcoma, and periosteal osteosarcoma (81,82,85–88). Histologically and radiologically, juxtacortical chondroma is quite similar to juxtacortical chondrosarcoma. Lesion size is often the best differentiating feature, with juxtacortical chondromas being almost invariably smaller (2–3 cm in size range, 2 cm average) than juxtacortical chondrosarcoma (size range, 3–14 cm, 5 cm average) (81,82,85).

Differentiating between juxtacortical chondrosarcoma and periosteal osteosarcoma can be challenging, particularly pathologically, and there has been much confusion in the literature. Periosteal osteosarcoma is characterized by the presence of periosteal reaction perpendicular to the cortex on radiographs, young patient age (10–25 years), diaphyseal location, and a neoplastic osteoblastic component at histologic analysis (86–88). Both lesions contain predominantly chondroblastic tissue histologically. Parosteal osteosarcoma may be radiologically similar to juxtacortical chondrosarcoma and occurs in a similar anatomic location (posterior distal femoral metaphysis) and in patients of similar age distribution (86). However, parosteal osteosarcoma usually has a stalk of attachment to the cortex and extensive osteoid. Little to no chondroid tissue is seen in parosteal osteosarcoma, which allows histologic differentiation between these lesions.

Myxoid Chondrosarcoma of Bone

Although myxoid degeneration is a common feature in conventional intramedullary chondrosarcoma, morphologically distinct myxoid chondrosarcoma of bone is not a well-established entity. However, myxoid chondrosarcoma has been reported to represent up to 12% of chondrosarcomas of bone and has also been referred to as chordoid sarcoma (4,89–93). Kilpatrick et al (89) reported the findings in two cases and reviewed the literature in 1997, identifying a total of six cases, including the two they reported. Cytogenetic analysis of myxoid chondrosarcoma of bone has demonstrated a reciprocal translocation between chromosomes 9 and 22, t (9; 22)(q22–31; q11–12) (4,91–94). This translocation has been well demonstrated in extraskeletal myxoid chondrosarcoma and provides evidence of the equivalence of these lesions (91–94).

Although only limited conclusions can be drawn from the small sample of reported cases, affected individuals are typically male adults (mean age, 49 years, with a range of 9–76 years), and half of the reported cases have occurred in the femur (89). Based on this small sample, it also appears that myxoid chondrosarcoma of bone has a more aggressive clinical course than conventional intramedullary chondrosarcoma, with patients commonly developing distant metastases and local recurrence (89). This aggressive behavior contrasts sharply with that of low-grade conventional chondrosarcoma, which rarely metastasizes in the absence of dedifferentiation (16).

The more aggressive clinical behavior is reflected in the radiologic appearance, with reported radiographic features including a permeative pattern of osseous destruction and an associated soft-tissue mass (Fig 16). In our experience, matrix mineralization is frequently apparent on CT scans but not extensive (Fig 16b). CT and MR imaging demonstrate the markedly high water content with low attenuation and very high signal intensity with T2-weighted pulse sequences, respectively (Fig 16). Unlike conventional chondrosarcoma, myxoid chondrosarcoma frequently contains hemorrhage, which appears as areas of high signal intensity with all MR pulse sequences, particularly in the large associated soft-tissue components (Fig 16). Enhancement after intravenous administration of contrast material is often only mild and septal to peripheral in pattern.

Mesenchymal Chondrosarcoma of Bone

Lichtenstein and Bernstein (95) first described mesenchymal chondrosarcoma of bone in 1959. It is an aggressive malignant cartilaginous neoplasm with a strong tendency to metastasize that accounts for 2%–13% of all chondrosarcomas of bone and 5% of all primary bone tumors that lead to biopsy (1–5,95–103). Skeletal lesions represent 25%–70% of mesenchymal chondrosarcomas (1–5,96). In one series, there were almost twice as many skeletal cases (65%) as extraskeletal cases (35%), and 7% of the osseous lesions were multicentric (96). Clinical symptoms are nonspecific and include pain, swelling, and a palpable soft-tissue mass. Men and women are equally affected, most frequently in the 2nd to 4th decade of life (average age, 25 years) (1–5,96).

In contradistinction to conventional chondrosarcomas, mesenchymal lesions most commonly involve the axial skeleton. The craniofacial region is most frequently affected (15%–30% of cases), specifically the mandible and maxilla (1–5,71). Other common sites include the femur (15%–23% of cases), ribs (12%–23%), spine (10%–14%), pelvis (10%–13%), humerus (4%–16%), tibia (4%–6%), and fibula (5%) (1–7,95–103). Although most cases arise in previously normal bone, mesenchymal chondrosarcoma may occur as a secondary lesion associated with preexisting fibrous dysplasia (97).

Imaging plays an important role in the management of mesenchymal chondrosarcoma, which has both similarities to other chondrosarcomas and differences (96–103). Radiographs usually show aggressive bone destruction, with a moth-eaten to permeative pattern and ill-defined periosteal reaction (95–102). The tumor is often very large, with extensive extraosseous components. Areas of characteristic ring-and-arc chondroid calcifications are seen in up to 67% of cases, although they are often not extensive (Fig 17) (4,95–103). Most of these tumors are centered in the medullary bone, but about 6% are surface lesions (96). Pathologic fractures occur infrequently (96).

CT typically shows aggressive bone destruction with a large associated soft-tissue mass and chondroid mineralization, as well as foci of central low attenuation (likely representing necrosis) (Fig 17). The tumors may appear to be heavily calcified on CT scans but more commonly show "finely stippled" calcification (98,102). At CT angiography, the lesions have less immediate enhancement than adjacent vascular structures, but prominent delayed enhancement may be seen (102,103).

MR imaging descriptions of mesenchymal chondrosarcoma are relatively few and often incomplete (98–103). In our experience, mesenchymal chondrosarcomas usually demonstrate nonspecific intrinsic features on MR images with low to intermediate signal intensity with T1-weighted pulse sequences and intermediate signal intensity with T2-weighted pulse sequences (Fig 17). Areas of matrix mineralization are often more difficult to detect on MR images than on CT scans. Mesenchymal chondrosarcoma shows

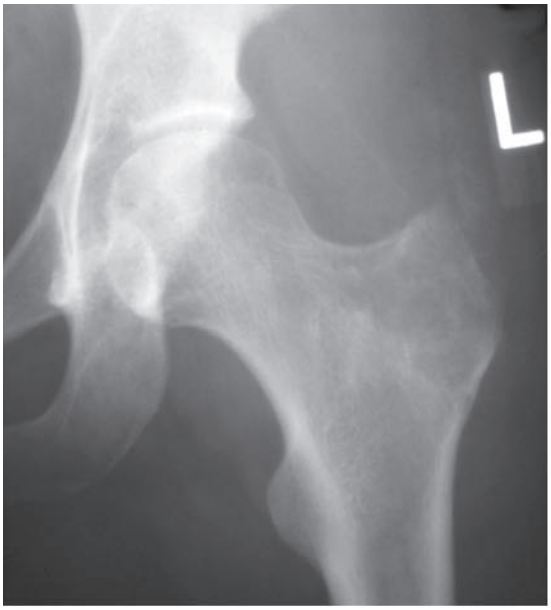

a.

Figure 16. Myxoid chondrosarcoma of bone in a 50-year-old woman with a gluteal mass. **(a)** Anteroposterior hip radiograph shows lytic destruction of the greater trochanter with faint sclerosis. **(b)** Axial CT scan shows aggressive bone destruction, subtle chondroid matrix mineralization in the intraosseous and extraosseous components (arrows), and marked low attenuation of a soft-tissue mass *(M)*. **(c)** Coronal T1-weighted (500/25) MR image reveals the low-signal-intensity mass *(M)* arising from the greater trochanter with a hemorrhagic focus superiorly *(H)*. **(d)** Axial T2-weighted (3,000/80) MR image reveals the marked high signal intensity of the mass *(M)*. Matrix mineralization cannot be seen on the MR images. **(e)** Photograph of the axially sectioned gross specimen corresponds well with the imaging features, as it demonstrates high-water-content myxoid and cartilaginous nodules *(M)*, hemorrhage *(H)*, and chondroid mineralization (arrows) in the mass extending out of the greater trochanter.

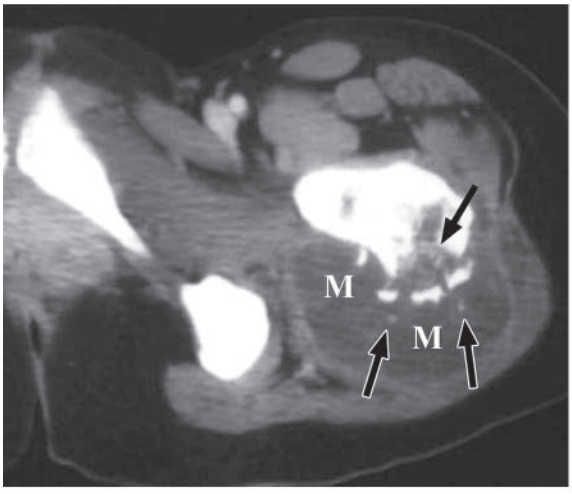

b.

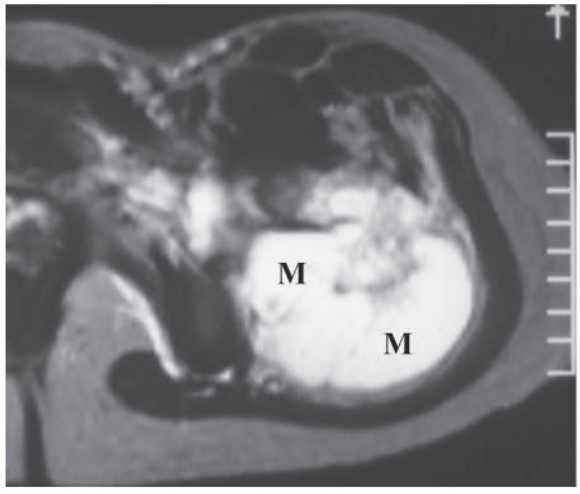

d.

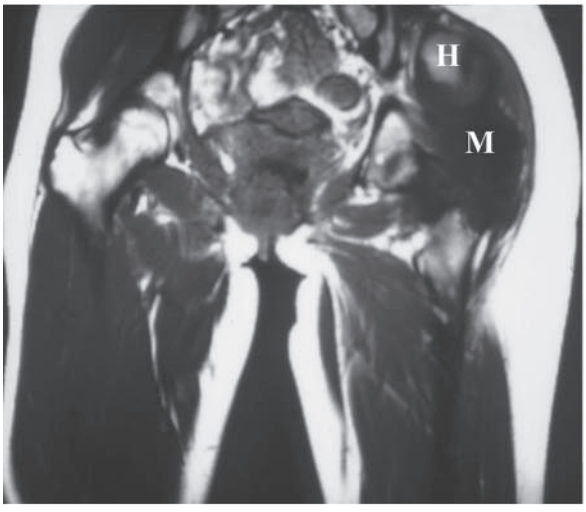

c.

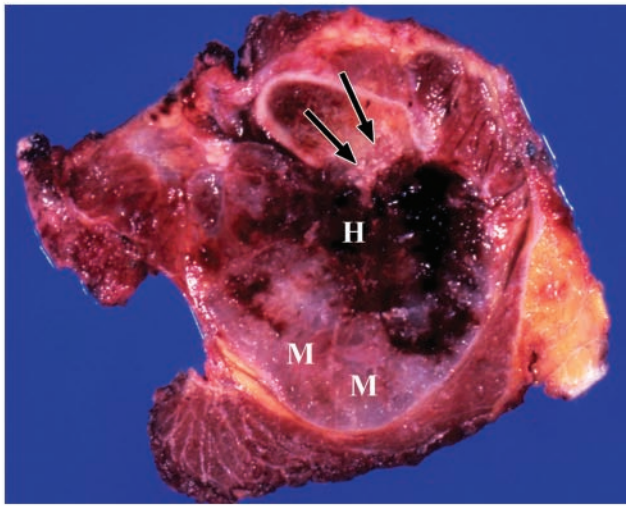

e.

Figure 17. Mesenchymal chondrosarcoma of the acromion in a 30-year-old man with right shoulder pain for 1 year. **(a)** Anteroposterior shoulder radiograph shows a lesion with expansile remodeling of the acromion and relatively subtle chondroid calcifications (arrows). **(b)** Axial CT scan reveals abundant chondroid matrix that replaces the acromion. **(c–e)** Coronal T1-weighted (500/17) MR images before **(c)** and after **(d)** intravenous gadolinium administration demonstrate an intraosseous and extraosseous mass *(M)* with intermediate signal intensity and moderate diffuse enhancement *(E)*. Prominent serpentine vascular structures (arrows) with high flow and feeding vessels (arrows) are seen on the contrast material–enhanced image **(d)** and the coronal T2-weighted (3,116/16) MR image with fat saturation **(e)**. Lesion shows heterogeneous intermediate signal intensity on the long repetition image. **(f)** Photograph of the gross specimen also shows the large scapular lesion arising from the acromion with several vascular channels identified (arrows).

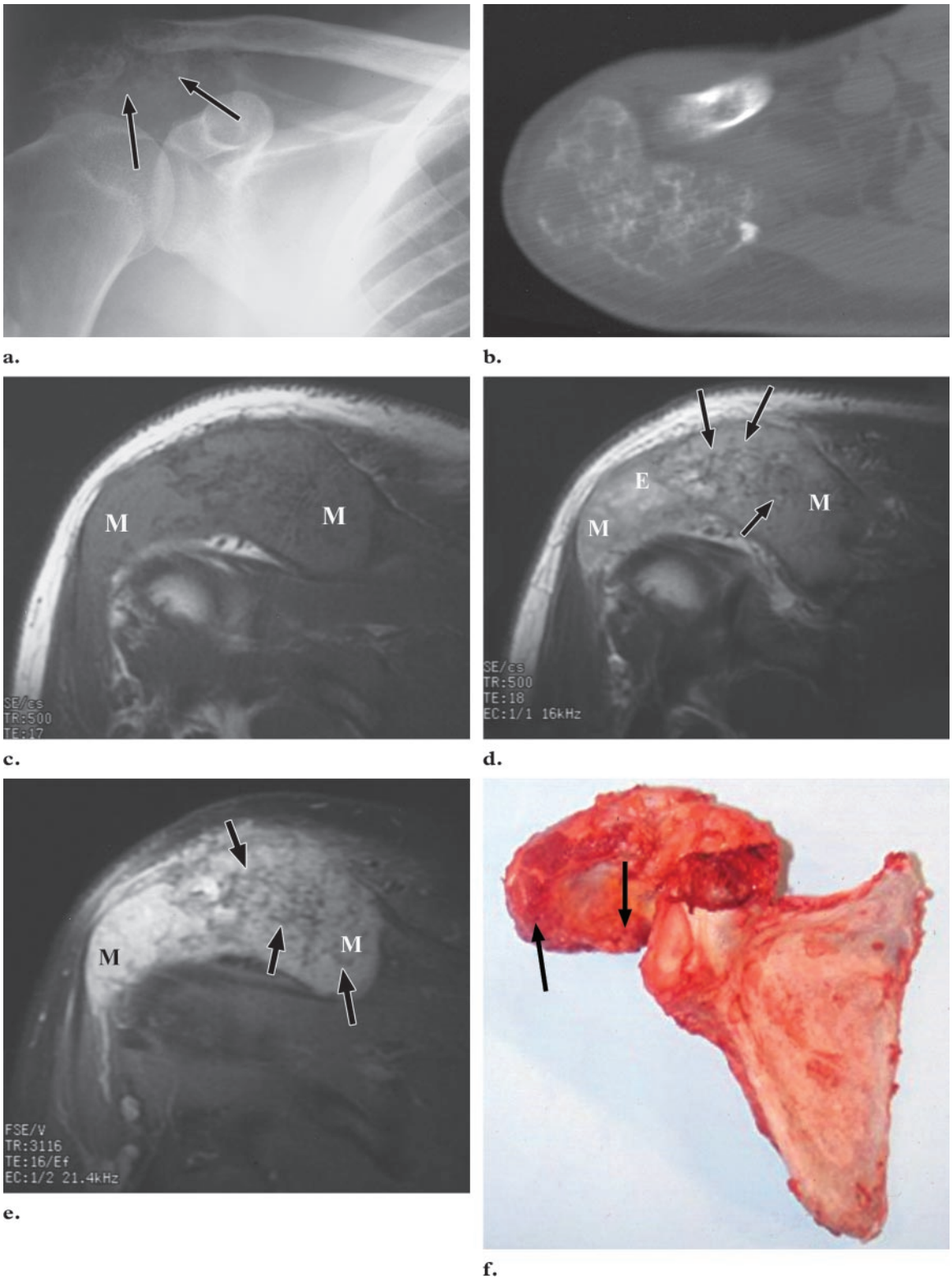

a different pattern of contrast enhancement compared with conventional chondrosarcoma on MR images (104). The pattern of enhancement varies from homogeneous to heterogeneous but is often diffuse and lacks the typical cartilaginous septal and peripheral enhancement (Fig 17d). Some lesions demonstrate low-signal-intensity, serpentine, high-flow vessels, a feature not seen in other chondrosarcomas (Fig 17d). The likely cause of these imaging manifestations is the pathologic components, with small cell regions and hemangiopericytoma-like areas intermixed with cartilaginous tissue.

Thus, the diagnosis of mesenchymal chondrosarcoma of bone is suggested by an aggressive osseous lesion with subtle chondroid matrix mineralization and features of intermediate signal intensity on T2-weighted MR images (lower than those of conventional chondrosarcoma), with more dramatic enhancement on CT or MR images than expected with conventional chondrosarcoma.

Extraskeletal Chondrosarcoma

Extraskeletal chondrosarcomas are relatively rare neoplasms and are far less common than their intraosseous counterparts, representing approximately 2% of all soft-tissue sarcomas (105–116). The histologic types of lesions that account for extraskeletal chondrosarcoma are myxoid, mesenchymal, and very rarely low grade.

Extraskeletal myxoid chondrosarcoma is the most common histologic type of soft-tissue chondrosarcoma. It is a tumor of adults, with the mean age at presentation being approximately 50 years, although patient ages range from 4 to 92 years (108–113). There is a male predominance in most but not all series (108–113). The lesion is extremely rare in patients younger than 20 years of age (109). The vast majority of lesions arise in the extremities, with the thigh being the single most common location (108,110,113). Most lesions are in the deep soft tissue, but approximately 25%–33% are subcutaneous (Fig 18) (108–113).

Extraskeletal mesenchymal chondrosarcoma typically affects young adults between 15 and 35 years of age, with a female predilection (106,107). Lesions in soft tissue account for 30%–75% of all mesenchymal chondrosarcomas, although osseous sites predominate in most series (106, 107,114–116). Although many of these lesions affect the head and neck (brain, orbit, and meninges), musculoskeletal lesions most commonly involve the lower extremity (particularly the thigh) (97,99,106,107,115,116). Clinical symptoms of both extraskeletal myxoid and mesenchymal chondrosarcomas are nonspecific, with the most common finding being a slowly enlarging painless soft-tissue mass.

Radiographs of these lesions often demonstrate a nonspecific soft-tissue mass. Areas of chondroid matrix mineralization may be apparent, and this finding is much more frequent in mesenchymal chondrosarcoma. In the series by Shapeero et al (99), four of seven lesions (57%) showed chondroid mineralization on radiographs or CT scans. In our experience, matrix mineralization is more frequent than has been described in the literature (Fig 18). Underlying bone erosion or invasion and periosteal reaction are unusual but may be seen.

On CT and MR images, both myxoid and mesenchymal chondrosarcomas have features similar to those described for tumors of these histologic types located in bone. Extraskeletal myxoid chondrosarcoma, reflective of its extremely high water content, appears with low attenuation

Figure 18. Extraskeletal myxoid chondrosarcoma in a 50-year-old woman with a slowly enlarging painless soft-tissue mass of the right gluteus region. **(a)** Oblique hip radiograph demonstrates a large soft-tissue mass with calcifications. **(b)** Axial CT scan shows the intramuscular low-attenuation soft-tissue mass *(M)* of the right gluteus maximus with prominent calcifications (arrows). **(c, d)** Axial MR images also reveal the large soft-tissue mass *(M)* that has low signal intensity with T1-weighting (550/10) **(c)** and heterogeneous high signal intensity with T2-weighting (3,000/75) **(d)** without depiction of the calcification. **(e)** Photograph of the axially sectioned gross specimen reveals the soft-tissue myxoid chondrosarcoma with central necrosis (*).

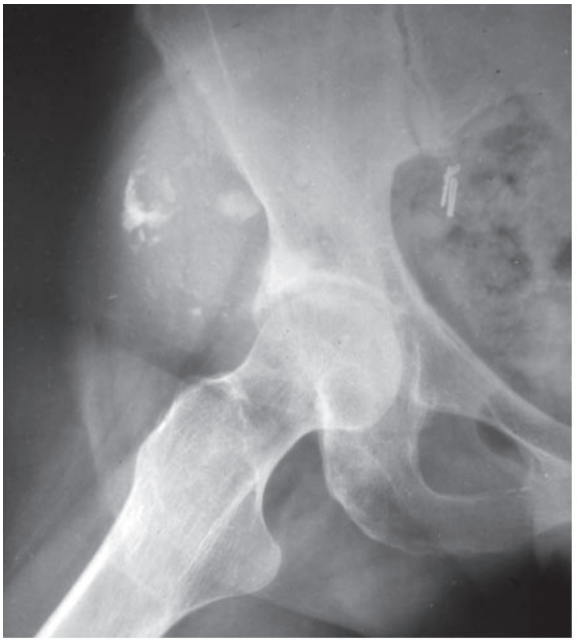

a.

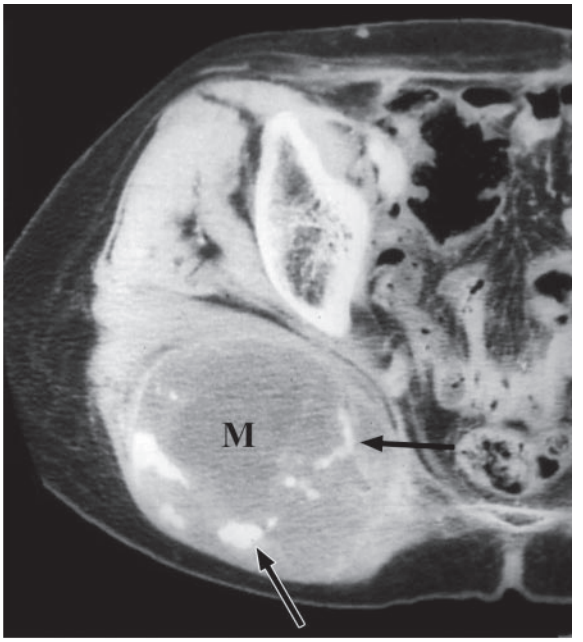

b.

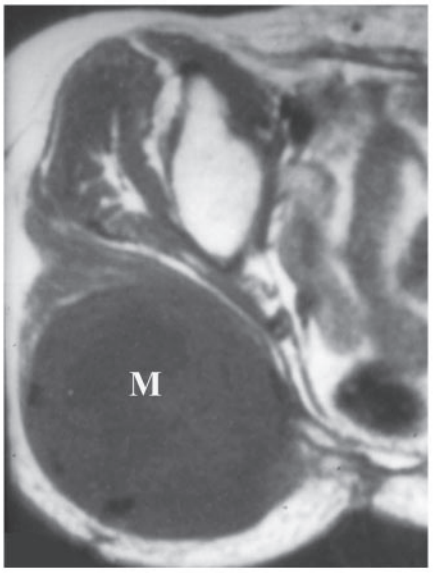

c.

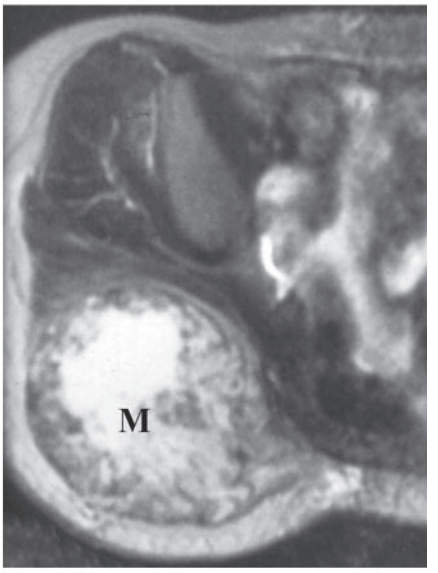

d.

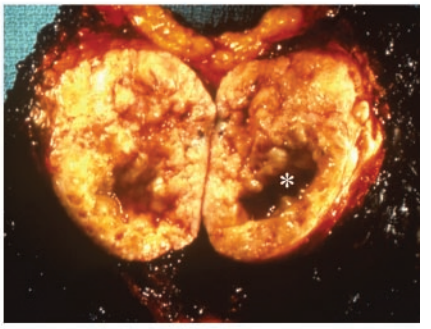

e.

on CT scans and very high signal intensity on T2-weighted MR images, with only mild peripheral to septal enhancement after contrast material administration (Fig 18). Extraskeletal mesenchymal chondrosarcoma, which has lower water content caused by the intermixture of small cells and more limited cartilaginous tissue, has attenuation similar to that of muscle on CT scans and typically has intermediate signal intensity on T2-weighted MR images. Areas of necrosis may be seen, appearing as areas of high signal intensity on T2-weighted MR images. MR images obtained after intravenous administration of contrast material reveal prominent, diffuse but heterogeneous enhancement, and in our experience, serpentine high-flow vessels may be seen, findings that are related to the hemangiopericytoma-like areas identified histologically with extraskeletal mesenchymal chondrosarcoma.

Dedifferentiated Chondrosarcoma

Dahlin and Beabout (117) originally described dedifferentiated chondrosarcoma in 1971, and the lesion has also been referred to as spindle cell chondrosarcoma. Most series agree that dedifferentiated chondrosarcomas constitute approximately 9%–10% of all chondrosarcomas and represent 1%–2% of all primary bone tumors that lead to biopsy (1–5). Mirra (2) suggests that dedifferentiation occurs in 10%–20% of conventional chondrosarcomas.

At least three mechanisms for the origin of dedifferentiated chondrosarcoma have been hypothesized. The most frequent theory is that the high-grade noncartilaginous component arises in a longstanding lower-grade chondrosarcoma. A second hypothesis is that the noncartilaginous sarcoma results from malignant transformation in an inflamed fibrous pseudocapsule of a lower-grade chondrosarcoma. Finally, the third theory is the possibility that malignant cell lines arise simultaneously in a chondrosarcoma with differing ability to differentiate (117–123).

Patients with dedifferentiated chondrosarcoma are older than those with conventional lesions; they are usually between 50 and 70 years old, with an average age of approximately 60 years (117–123). Men and women are affected equally. Patients present most frequently with pain (85% of cases), followed by pathologic fracture (31%) and soft-tissue mass (29%) (117–120).

The majority of lesions occur centrally in the medullary bone, although there are reports of dedifferentiation in juxtacortical chondrosarcoma. Sites of involvement parallel those of conventional intramedullary chondrosarcoma, with common locations including the femur (35% of cases), pelvis (29%), humerus (16%), scapula (6%), rib (6%), and tibia (5%) (1–5,117–123).

Imaging findings vary, depending on the proportion of conventional chondrosarcoma that has transformed to a noncartilaginous high-grade malignancy. When the proportion of high-grade lesion is small, the lesion may appear identical to a low-grade chondrosarcoma with an elongated multilobulated osteolytic lesion, cortical thickening, and endosteal scalloping containing "rings and arcs" of chondroid calcification (Fig 19a). As the high-grade noncartilaginous focus increases in size, there is a progression of aggressive bone lysis and a decrease in matrix mineralization. Associated soft-tissue masses, often large, are almost invariably seen.

CT and MR imaging may reveal two distinct areas with differing intrinsic characteristics. The low-grade conventional chondrosarcomatous elements have the previously described low attenuation on CT scans and very high signal intensity on T2-weighted MR images. The high-grade noncartilaginous component most frequently shows soft-tissue attenuation on CT scans (isoattenuated relative to muscle) and variable signal intensity on T2-weighted MR images ranging from low

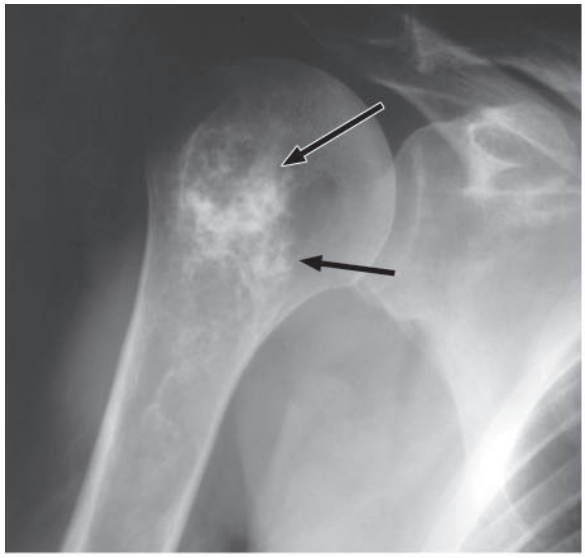

a.

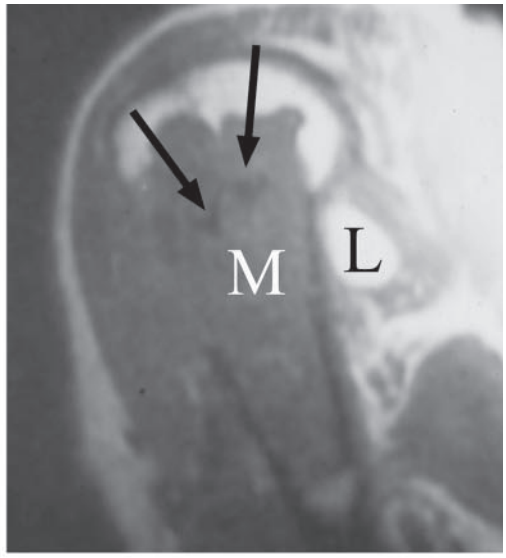

b.

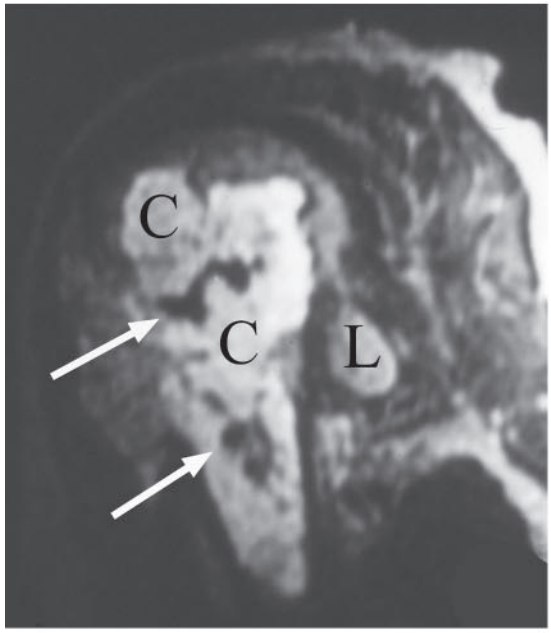

c.

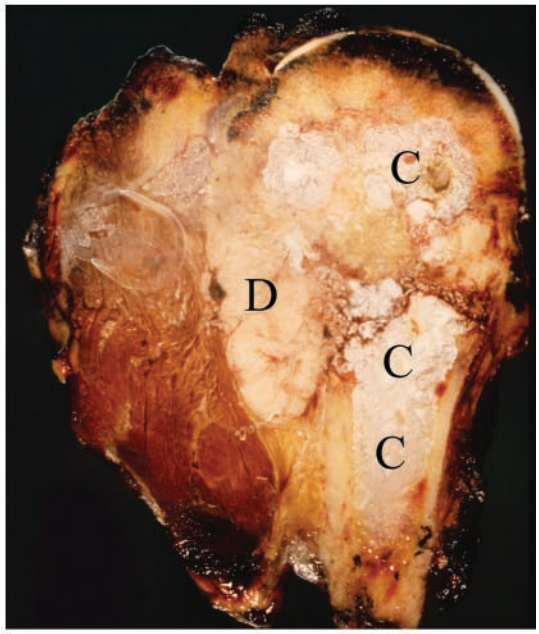

d.

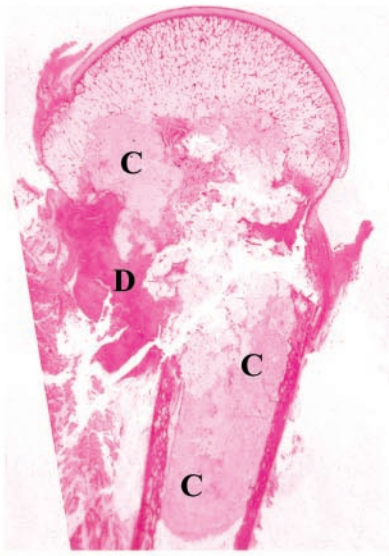

e.

Figure 19. Dedifferentiated chondrosarcoma of the humerus in a 79-year-old man with persistent right shoulder pain for several months. **(a)** Anteroposterior shoulder radiograph demonstrates a lytic lesion of the proximal humeral metaphysis with typical chondroid mineralization (arrows). **(b)** Sagittal T1-weighted (550/20) MR image reveals heterogeneous marrow replacement *(M)* with foci of decreased signal intensity corresponding to calcifications (arrows). **(c)** Sagittal T2-weighted (3,000/80) MR image demonstrates the high-signal-intensity cartilaginous component in bone *(C)* with lobular growth superiorly and foci of decreased intraosseous signal intensity corresponding to calcifications (arrows). There is a dedifferentiated component of the lesion anteriorly that is aggressively destroying the cortex and extending into the soft tissue and that has low to intermediate signal intensity with T2-weighting. An incidental lipoma *(L)* is seen anteriorly on both MR images. **(d, e)** Photographs of the coronally sectioned gross specimen and of the coronally sectioned whole-mounted specimen (hematoxylin-eosin stain) correlate identically with the MR images. The specimens reveal the low-grade cartilaginous component *(C)* in bone as well as a pale yellow portion of the lesion destroying cortex and extending into soft tissue *(D)*, which represents the high-grade dedifferentiated noncartilaginous component (malignant fibrous histiocytoma) of the lesion.

to high (although lower in signal intensity than the conventional chondrosarcomatous component) (Fig 19). Images obtained with intravenous contrast material demonstrate typical mild septal and peripheral enhancement in the lower-grade chondrosarcomatous component as opposed to prominent diffuse enhancement in the high-grade noncartilaginous areas. MR imaging is superior to CT in the differentiation between these two tissue types, owing to its improved contrast resolution, and is helpful for directing biopsy in these areas. In our experience, the soft-tissue mass is more likely than the intraosseous component to harbor the high-grade areas of the neoplasm (Fig 19).

Treatment and Prognosis

Conventional Intramedullary Chondrosarcoma

There is debate over the pathologic and radiologic criteria used to differentiate low-grade chondrosarcoma (grade 1) from active enchondroma. The term *low-grade chondrosarcoma* generally implies a locally aggressive tumor with limited capacity to metastasize to distant organs. There are two choices for surgical treatment for "low-grade" chondrosarcoma (grade 1) (124–130). The first is intralesional curettage, adjunct chemical or thermal ablation, and cementation or bone grafting of the defect. The second surgical option is wide excision with structural graft or metal reconstruction.

The decision on which form of treatment is most appropriate is complicated by tumor heterogeneity related to intermixture of intermediate- or high-grade neoplasm with low-grade tumor and variation in histopathologic interpretation. Sometimes, biopsy of cartilaginous lesions is only reluctantly performed because of two concerns. The first is failure to recognize higher-grade areas (grades 2–3), as is possible when needle or limited open biopsy is used and when representative tissue from these often large heterogeneous lesions is not obtained. The second concern is the possibility of spreading the often gelatinous tumor tissue along the biopsy tract. However in our opinion and experience, both of these issues can be adequately addressed and thus allow successful biopsy. First, biopsy should always be directed at the more aggressive areas of endosteal scalloping and the soft-tissue components or more diffusely enhancing regions (these areas usually show limited to no matrix mineralization) apparent in the vast majority of chondrosarcomas. These are the areas most likely to harbor higher-grade tumor foci. The spread of tumor along the biopsy tract is theoretically possible, although the prevalence must be exceedingly low and not well documented in the scientific literature (to the best of our knowledge). In addition, the biopsy tract is typically resected with the surgical excision.

Acceptable oncologic and functional results have been observed in patients with grade 1 chondrosarcoma treated with curettage and cryosurgery alone (126,127), because the rate of metastatic disease has been variably reported as nonexistent or very low. However, local recurrence is not unusual if there is inadequate resection

(126,127). Large lesions and chondrosarcomas in anatomic locations that do not allow adequate margins or complete excision (such as the spine, craniofacial region, ribs, pelvis) have an obvious increased risk of local recurrence and metastatic disease (10,128,129). These local recurrences can ultimately lead to patient demise. In addition, 10% of local recurrences are associated with higher-grade histologic characteristics (1–5). Most local recurrences become evident in the first 5 years after initial treatment. The decision to perform an intralesional resection for a suspected low-grade chondrosarcoma depends on critical evaluation of preoperative imaging studies (124–130). In patients with grade 1 conventional chondrosarcoma with deep endosteal scalloping, an intact cortical rim, and no soft-tissue mass, we advocate an intralesional procedure. Internal fixation with plates and screws is necessary to prevent pathologic fracture, because of the significant stress riser created when the tumor is adequately removed.

Conventional chondrosarcomas that demonstrate foci of cortical destruction resulting from deep endosteal scalloping (with or without a soft-tissue mass) or those lesions with obvious histologic grade 2 or 3 features in biopsy specimens all require wide local excision to achieve tumor free margins. Aggressive surgical management is necessary to optimize local disease control and reduce the frequency of metastatic spread of disease (128,129). Indeed, this is reflected in both the rates of local recurrence and distant metastases. Local recurrence is 9.5% when there is adequate initial resection for grades 1 and 2 chondrosarcoma versus 93% when only local marginal excision or curettage is performed (4,16,129). The local recurrence rate of grade 3 chondrosarcoma is 47% (4,16). The reported rate of distant metastases is 10%–50% for grade 2 lesions and 50%–71% for grade 3 lesions (4,16). Metastases most commonly involve the lung, regional lymph nodes, and liver. These facts emphasize our belief that although the controversy concerning differentiation of grade 1 conventional chondrosarcoma versus enchondroma of long bone continues, the more important distinction is identifying grade 2 or grade 3 chondrosarcomas for purposes of treatment and prognosis implications. In our experience, imaging features allow this differentiation because higher-grade chondrosarcomas (grade 2 or 3) invariably cause cortical destruction and are commonly associated with soft-tissue masses. These findings are in contrast to those associated with symptomatic, intramedullary cartilage tumors of long bones that cause endosteal scalloping of less than two-thirds of the cortex. These latter lesions can be safely followed at 4- to 6-month intervals for 2 years, then annually for up to 5 years. The overall 5-year survival rates for chondrosarcoma are 90%–94% (grade 1), 61%–81% (grade 2), and 43%–44% (grade 3), whereas the 10-year survival rates are 83%–87% (grade 1), 41%–64% (grade 2), and 27%–29% (grade 3) (2–4,16,130).

Clear Cell Chondrosarcoma

Clear cell chondrosarcoma, although a low-grade tumor, is often inadequately treated initially with curettage only because of its epiphyseal location. This location suggests the diagnosis of chondroblastoma, and malignancy is often not suspected. This form of therapy invariably leads to recurrence, whereas adequate aggressive initial surgical resection with joint arthroplasty is usually curative. The diagnosis must be clinically suspected before biopsy is performed to avoid joint contamination. Overall recurrence rate is 16%, and approximately 15% of patients die of the disease. Metastases to the lung, brain, and bones have been reported (1–5,72).

Juxtacortical Chondrosarcoma

Treatment of juxtacortical chondrosarcoma is wide surgical resection. Local recurrence and metastatic disease have been reported, but the prevalence is low, even with higher-grade lesions (2–4,80). Dedifferentiation has been reported and is associated with an ominous prognosis (84,131).

Myxoid Chondrosarcoma

Both extraskeletal and intraosseous myxoid chondrosarcomas can be considered intermediate-grade tumors, with initial wide local resection being the treatment of choice. The most frequent metastatic sites are the lungs and regional lymph nodes. Metastases may occur after a long delay. Patients with intraosseous lesions have a 5-year survival rate of 60%, which decreases to 20% at 25 years (4). Patients with extraskeletal myxoid chondrosarcoma have an estimated survival rate of 90% at 5 years, 70%–78% at 10 years, and 60% at 15 years (106–108). Factors that adversely affect the prognosis of patients with extraskeletal lesions include pleomorphism, high mitotic activity, proximal location of the lesion, older patient age, large tumor size, and metastases at presentation (106,107). High cellularity as a prognostic factor is controversial (107).

Mesenchymal Chondrosarcoma

Mesenchymal chondrosarcomas, both extraskeletal and intraosseous, are high-grade aggressive tumors that require wide local excision when possible. Local recurrence is common, as are metastases, which involve the lung, regional lymph nodes, and bone. Patients with intraosseous lesions have a 5-year survival rate of 42% and a 10-year survival rate of 28% (1–5,96). Patients with extraskeletal mesenchymal chondrosarcoma have an estimated survival rate of 55% at 5 years and 27% at 10 years (96,106,107).

Dedifferentiated Chondrosarcoma

Dedifferentiated chondrosarcoma is a highly lethal malignancy, despite adequate aggressive initial wide surgical resection or even amputation. Unfortunately, metastases occur early; are frequent; and commonly involve the lungs, lymph nodes, and viscera (1–5,117,118,132). It is the poorly differentiated component that metastasizes. The prognosis is dismal, with an estimated 5-year survival rate of less than 10%–25% (1–5,117,118,132). Most patients die within 2 years, and the median survival is less than 1 year.

Chemotherapy and Radiation Therapy

Chemotherapy and radiation therapy have limited roles in the overall treatment of chondrosarcoma (133,134). This is particularly true for conventional chondrosarcomas because these neoplasms are not generally considered to be significantly sensitive to these treatments. Radiation therapy may be employed for higher-grade conventional chondrosarcomas (grade 2 and 3) that are incompletely excised or in locations that are surgically inaccessible, such as the skull base (1–5). However, in patients with more aggressive chondrosarcomas such as mesenchymal and dedifferentiated lesions, both of these neoadjuvant therapies are often used to control local disease and to decrease the risk of metastases. Chemotherapy has also been used to treat clear cell chondrosarcoma (72–77). Radiation therapy (6,000 cGy) has been employed to treat extraskeletal myxoid chondrosarcoma, which is resistant to chemotherapy (106,107,133). Chemotherapy is generally given before definitive surgical resection, and follow-up imaging (usually MR imaging) is used to assess tumor response. The chemotherapeutic regimens are similar to those used for osteosarcoma and include methotrexate, adriamycin, cis-platinum, and ifosfamide. Experimental work on the effect of fluoroquinolones on malignant cartilage lesions has been encouraging in vitro, although potential clinical efficacy has not been demonstrated (134).

Conclusions

Primary chondrosarcoma is the third most common primary malignant tumor of bone, representing 20%–27% of primary malignant osseous neoplasms. Its radiologic manifestations have a wide spectrum of appearances. We have reviewed, illustrated, and correlated the radiologic and pathologic features of the various types of primary chondrosarcoma, including conventional intramedullary, clear cell, juxtacortical, myxoid, mesenchymal, extraskeletal, and dedifferentiated.

Although the pathologic appearance varies with specific lesion type, chondrosarcomas grow with lobular type architecture, and these hyaline cartilage nodules demonstrate high water content and peripheral enchondral ossification. The radiographic appearances of these lesions reflect these pathologic features and are often characteristic, with typical ring-and-arc chondroid matrix mineralization (representing the enchondral ossification) and aggressive features of deep endosteal scalloping and soft-tissue extension. CT optimally depicts the matrix mineralization, particularly when it is subtle or in lesions located in complex anatomic areas. CT and MR imaging depict the high water content seen in conventional, juxtacortical, and myxoid chondrosarcomas as low attenuation and very high signal intensity with T2-weighted pulse sequences, respectively. High-grade chondrosarcomas such as mesenchymal and dedifferentiated lesions often contain areas of matrix mineralization that suggest a chondroid neoplasm on radiographs but also show aggressive patterns of bone destruction and large associated soft-tissue masses. Additional features on CT and MR images of soft-tissue attenuation, intermediate signal intensity with T2-weighted pulse sequences, and more prominent and diffuse contrast enhancement frequently suggest these more aggressive types of chondrosarcoma. Understanding and recognizing the spectrum of appearances of the various types of primary chondrosarcoma allow improved patient assessment and are vital for optimal clinical management, including diagnosis, biopsy, staging, treatment, and expectations for prognosis.

Acknowledgments: The authors gratefully acknowledge the support of Anika Ismel Torruella for manuscript preparation. In addition, we thank the residents who attend the Armed Forces Institute of Pathology's radiologic-pathology courses (past, present, and future) for their contribution to our series of patients: Without them, this project would not have been possible.

References

1. Resnick D, Kyriakos M, Greenway GD. Tumors and tumor-like lesions of bone: imaging and pathology of specific lesions. In: Resnick D, ed. Diagnosis of bone and joint disorders. 4th ed. Philadelphia, Pa: Saunders, 2002; 3897–3920.
2. Mirra JM. Intramedullary cartilage and chondroid-producing tumors. In: Mirra JM, ed. Bone tumors: clinical, radiologic, and pathologic correlations. Philadelphia, Pa: Lea & Febiger, 1989; 439–535.
3. Dorfman HD, Czerniak B. Malignant cartilage tumors. In: Gery L, ed. Bone tumors. St Louis, Mo: Mosby, 1998; 353–411.
4. Huvos AG. Chondrosarcoma including spindle-cell (dedifferentiated) and myxoid chondrosarcoma: mesenchymal chondrosarcoma. In: Mitchell J, ed. Bone tumors: diagnosis, treatment, and prognosis, 2nd ed. Philadelphia, Pa: Saunders, 1991; 343–393.
5. Jaffe HL. Tumors and tumorous conditions of the bones and joints. Philadelphia, Pa: Lea & Febiger, 1958; 315–340.
6. Lichtenstein L, Jaffe HL. Chondrosarcoma of the bone. Am J Pathol 1943; 19:553–589.
7. Hudson TH, Moser RP Jr, Gilkey FW, Aoki J. Chondrosarcoma. In: Moser RP Jr, ed. Cartilaginous tumors of the skeleton. Philadelphia, Pa: Hanley & Belfus, 1990; 155–205.
8. Rozeman LB, Hogendoorn PC, Bovee JV. Diagnosis and prognosis of chondrosarcoma of bone. Expert Rev Mol Diagn 2002; 2:461–472.
9. Aigner T. Towards a new understanding and classification of chondrogenic neoplasias of the skeleton: biochemistry and cell biology of chondrosarcoma and its variants. Virchows Arch 2002; 441:219–230.
10. Pring ME, Weber KL, Unni KK, Sim FH. Chondrosarcoma of the pelvis: a review of sixty-four cases. J Bone Joint Surg Am 2001; 11:1630–1642.
11. Marco RA, Gitelis S, Brebach GT, Healey JH. Cartilage tumors: evaluation and treatment. J Am Acad Orthop Surg 2000; 8:292–304.
12. Somers J, Faber LP. Chondroma and chondrosarcoma. Semin Thorac Cardiovasc Surg 1999; 11:270–277.
13. Murphey MD, Flemming DJ, Boyea SR, Bojescul JA, Sweet DE, Temple HT. Enchondroma versus chondrosarcoma in the appendicular skeleton: differentiating features. RadioGraphics 1998; 18:1213–1245.
14. Brien EW, Mirra JM, Kerr R. Benign and malignant cartilage tumors of bone and joint: their anatomic and theoretical basis with an emphasis on radiology, pathology, and clinical biology. I. The intramedullary cartilage tumors. Skeletal Radiol 1997; 26:325–353.

15. Campanacci M. Bone and soft tissue tumors. New York, NY: Springer-Verlag, 1991; 1–1131.
16. Evans HL, Ayala AG, Romsdahl MM. Prognostic factors in chondrosarcoma of bone: a clinicopathologic analysis with emphasis on histologic grading. Cancer 1977; 40:818–831.
17. Mirra JM, Gold R, Downs J, Eckardt JJ. A new histologic approach to the differentiation of enchondroma and chondrosarcoma of the bones: a clinicopathologic analysis of 51 cases. Clin Orthop 1985; 201:214–237.
18. Mulder JD, Kroon HM, Schutte HE, Taconis WK, eds. Radiologic atlas of bone tumors. Amsterdam, the Netherlands: Elsevier, 1993; 377–421.
19. Sanerkin NG. The diagnosis and grading of chondrosarcoma of bone: a combined cytologic and histologic approach. Cancer 1980; 45:582–594.
20. Unni KK. Enchondroma and chondrosarcoma. In: Unni KK, ed. Dahlin's bone tumors: general aspects and data on 11,087 cases. 5th ed. Philadelphia, Pa: Lippincott-Raven, 1996; 71–109.
21. Flemming DJ, Murphey MD. Enchondroma and chondrosarcoma. Semin Musculoskelet Radiol 2000; 4:59–71.
22. Geirnaerdt MJ, Hermans J, Bloem JL, et al. Usefulness of radiology in differentiating enchondroma from central grade I chondrosarcoma. AJR Am J Roentgenol 1997; 169:1097–1104.
23. Hudson TM, Manaster BJ, Springfield DS, Spanier SS, Enneking WF, Hawkins IF Jr. Radiology of medullary chondrosarcoma: preoperative treatment planning. Skeletal Radiol 1983; 10:69–78.
24. Lodwick GS, Wilson AF, Farrell C, Virtama P, Ditrich F. Determining growth rates of focal lesions of bone from radiographs. Radiology 1980; 34:577–583.
25. Lodwick GS. The radiologist's role in the management of chondrosarcoma (editorial). Radiology 1984; 150:275.
26. Preidler KW, Brossmann J, Daenen B, et al. Measurements of cortical thickness in experimentally created endosteal bone lesions: a comparison of radiography, CT, MR imaging, and anatomic sections. AJR Am J Roentgenol 1997; 168:1501–1505.
27. Reiter FB, Ackerman LV, Staple TW. Central chondrosarcoma of the appendicular skeleton. Radiology 1972; 105:525–530.
28. Ragsdale BD, Sweet DE, Vinh TN. Radiology as gross pathology in evaluating chondroid lesions. Hum Pathol 1989; 20:930–951.
29. Rosenthal DI, Schiller AL, Mankin HJ. Chondrosarcoma: correlation of radiological and histological grade. Radiology 1984; 150:21–26.
30. Sweet DE, Madewell JE, Ragsdale BD. Radiologic and pathologic analysis of solitary bone lesions. III. Matrix patterns. Radiol Clin North Am 1981; 19:785–814.
31. West OC, Reinus WR, Wilson AJ. Quantitative analysis of the plain radiographic appearance of central chondrosarcoma of bone. Invest Radiol 1995; 30:440–447.
32. Hudson TM, Chew FS, Manaster BJ. Radionuclide bone scanning of medullary chondrosarcoma. AJR Am J Roentgenol 1982; 139:1071–1076.
33. Kobayashi H, Lotoura Y, Hosono M, et al. Diagnostic value of Tc-99m (V) DMSA for chondrogenic tumors with positive Tc-99m HMDP uptake on bone scintigraphy. Clin Nucl Med 1995; 20:361–364.
34. Aoki J, Watanabe H, Shinozaki T, et al. FDG PET of primary benign and malignant bone tumors: standardized uptake value in 52 lesions. Radiology 2001; 219:774–777.
35. Feldman F, van Heertum R, Manos C. FDG PET scanning of benign and malignant musculoskeletal lesions. Skeletal Radiol 2003; 32:201–208.
36. Dehdashti F, Siegel BA, Griffeth LK, et al. Benign versus malignant intraosseous lesions: discrimination by means of PET with 2-(F-18) fluoro-2-deoxy-D-glucose. Radiology 1996; 200: 243–247.
37. Dietlein M, Feaux de Lacroix W, Neufang KF, Steinbrich W, Schmidt J. Assessment of the grading of cartilaginous tumors of the long tubular bones from the radiologic and pathologic viewpoint. Rontgenblatter 1990; 43:74–180. [German]
38. Crim JR, Seeger LL. Diagnosis of low-grade chondrosarcoma. Radiology 1993; 189:503–504.
39. Mayes GB, Wallace S, Bernardino ME. Computed tomography of chondrosarcoma. J Comput Tomogr 1981; 5:345–348.
40. Moser RP Jr, Gilkey FW, Madewell JE. Enchondroma. In: Moser RP Jr, ed. Cartilaginous tumors of the skeleton. Philadelphia, Pa: Hanley & Belfus, 1990; 8–35.
41. Aoki J, Sone S, Fujioka F, et al. MR of enchondroma and chondrosarcoma: rings and arcs of Gd-DTPA enhancement. J Comput Assist Tomogr 1991; 15:1011–1016.
42. De Beuckeleer LH, De Schepper AM, Ramon F. Magnetic resonance imaging in cartilaginous tumors: is it useful or necessary? Skeletal Radiol 1996; 25:137–141.
43. De Beuckeleer LH, De Schepper AM, Ramon F, Somville J. Magnetic resonance imaging in cartilaginous tumors: a retrospective study of 79 patients. Eur J Radiol 1995; 21:34–40.
44. Geirnaerdt MJ, Bloem JL, Eulderink F, Hogendoorn PC, Taminiau AH. Cartilaginous tumors: correlation of gadolinium-enhanced MR imaging and histopathologic findings. Radiology 1993; 186:813–817.
45. Geirnaerdt MJ, Bloem JL, Van Der Woode H, Taminiau AH, Hogendoorn PC. Fast dynamic contrast-enhanced subtraction MR imaging allows differentiation of benign and low-grade malignant cartilaginous tumors (abstr). Radiology 1996; 201(P):359.
46. Janzen L, Logan PM, O'Connell JX, Connell DG, Munk PL. Intramedullary chondroid tumors of bone: correlation of abnormal peritumoral marrow and soft-tissue MRI signal with tumor type. Skeletal Radiol 1997; 26:100–106.
47. Varma DG, Ayala AG, Carrasco CH, et al. Chondrosarcoma: MR imaging with pathologic correlation. RadioGraphics 1992; 12:687–704.

48. Walker CW, Moore TE. MR imaging of hyaline cartilage-containing tumors. Appl Radiol 1998; April:20–26.
49. Yaghmai I. Angiographic features of chondromas and chondrosarcomas. Skeletal Radiol 1978; 3:91–98.
50. Lagergren C, Linbom A, Soderberg G. The blood vessels of chondrosarcomas. Acta Radiol 1961; 55:321–328.
51. Huvos AG, Marcove RC. Chondrosarcoma in the young: a clinicopathologic analysis of 79 patients younger than 21 years of age. Am J Surg Pathol 1987; 11:930–942.
52. McAfee MK, Pairolero PC, Bergstralh EJ, et al. Chondrosarcoma of the chest wall: factors affecting survival. Ann Thorac Surg 1985; 40:535–541.
53. Meyer CA, White CS. Cartilaginous disorders of the chest. RadioGraphics 1998; 18:1109–1123.
54. Vieta JO, Maier HC. Tumors of the sternum. Int Abstr Surg 1962; June:513–525.
55. Pascuzzi CA, Dahlin DC, Clagett OT. Primary tumors of the ribs and sternum. Surg Gynecol Obstet 1957; April:390–400.
56. Shin MS, Berland LL, Ho K. Computed tomography evaluation of primary and secondary sternal neoplasms. J Comput Tomogr 1986; 10:27–32.
57. Martini N, Huvos AG, Smith J, Beattie EJ Jr. Primary malignant tumors of the sternum. Surg Gynecol Obstet 1974; 138:391–395.
58. Nigrisoli M, Ferraro A, DeCristofaro R, Picci P. Chondrosarcoma of the hand and foot. Chir Organi Mov 1990; 75:315–323.
59. Cawte TG, Steiner GC, Beltran J, Dorfman HD. Chondrosarcoma of the short tubular bones of the hands and feet. Skeletal Radiol 1998; 27:625–632.
60. Crim JR, Mirra JM. Enchondroma protuberans. Skeletal Radiol 1990; 19:431–434.
61. Camins MB, Duncan AW, Smith J, Marcove RC. Chondrosarcoma of the spine. Spine 1978; 3:202–209.
62. Hermann G, Sacher M, Lanzieri CF, Anderson PJ, Rabinowitz JG. Chondrosarcoma of the spine: an unusual radiographic presentation. Skeletal Radiol 1985; 14:178–183.
63. Hirsh LF, Thanki A, Spector HB. Primary spinal chondrosarcoma with eighteen-year follow-up: case report and literature review. Neurosurgery 1984; 14:747–749.
64. Murphey MD, Andrews CL, Flemming DJ, Temple HT, Smith WS, Smirniotopoulos JG. Primary tumors of the spine: radiologic-pathologic correlation. RadioGraphics 1996; 16:1131–1158.
65. Shives TC, McLeod RA, Unni KK, Schray MF. Chondrosarcoma of the spine. J Bone Joint Surg Am 1989; 71:1158–1165.
66. Kothary N, Law M, Cha S, Zagzag D. Conventional and perfusion MR imaging of parafalcine chondrosarcoma. AJNR Am J Neuroradiol 2003; 24:245–248.
67. Rosenberg AE, Nielsen GP, Keel SB, et al. Chondrosarcoma of the skull base: a clinicopathologic study of 200 cases with emphasis on its distinction from chordoma. Am J Surg Pathol 1999; 23:1370–1378.
68. Neff B, Sataloff RT, Sorey L, Hawkshaw M, Spiegel JR. Chondrosarcoma of the skull base. Laryngoscope 2002; 112:134–139.
69. Crockard HA, Cheeseman A, Steel T, et al. A multidisciplinary team approach to skull base chondrosarcomas. J Neurosurg 2001; 95:184–189.
70. Schmidinger A, Rosahl SK, Vorkapic P, Samii M. Natural history of chondroid skull base lesion: case report and review. Neuroradiology 2002; 44:268–271.
71. Huvos AG. Chondrosarcoma of the craniofacial bones. In: Mitchell J, ed. Bone tumors: diagnosis, treatment, and prognosis. 2nd ed. Philadelphia, Pa: Saunders, 1991; 395–403.
72. Unni KK, Dahlin DC, Beabout JW, Sim FH. Chondrosarcoma: clear-cell variant—a report of sixteen cases. J Bone Joint Surg Am 1976; 58:676–683.
73. Kumar R, David R, Cierney G 3rd. Clear cell chondrosarcoma. Radiology 1985; 154:45–48.
74. Bagley L, Kneeland JB, Dalinka MK, Bullough P, Brooks J. Unusual behavior of clear-cell chondrosarcoma. Skeletal Radiol 1993; 22:279–282.
75. Kaim AH, Hugli R, Bonel HM, Jundt G. Chondroblastoma and clear-cell chondrosarcoma: radiological and MRI characteristics with histopathological correlation. Skeletal Radiol 2002; 31:88–95.
76. Present D, Bacchini P, Pignatti G, Picci P, Bertoni F, Campanacci M. Clear cell chondrosarcoma of bone: a report of 8 cases. Skeletal Radiol 1991; 20:187–191.
77. Bloem JL, Mulder JD. Chondroblastoma: a clinical and radiological study of 104 cases. Skeletal Radiol 1985; 14:1–9.
78. Lichtenstein L. Tumors of periosteal origin. Cancer 1955; 8:1060–1069.
79. Schajowicz F. Juxtacortical chondrosarcoma. J Bone Joint Surg Br 1977; 59:473–480.
80. Nojima T, Unni KK, McLeod RA, Pritchard DJ. Periosteal chondroma and periosteal chondrosarcoma. Am J Surg Pathol 1985; 9:666–677.
81. Robinson P, White LM, Sundaram M, et al. Periosteal chondroid tumors: radiologic evaluation with pathologic correlation. AJR Am J Roentgenol 2001; 177:1183–1188.
82. Bertoni F, Boriani S, Laus M, Campanacci M. Periosteal chondrosarcoma and periosteal osteosarcoma: two distinct entities. J Bone Joint Surg Br 1982; 64:370–376.
83. Zenmyo M, Komiya S, Nakashima M, Irie K, Kakizoe M, Inoue A. Giant juxtacortical chondrosarcoma of the humerus. Orthopedics 2000; 23:497–498.
84. Kumta SM, Griffith JF, Chow LT, Leung PC. Primary juxtacortical chondrosarcoma dedifferentiating after 20 years. Skeletal Radiol 1998; 27:569–573.
85. Bauer TW, Dorfman HD, Latham JT Jr. Periosteal chondroma: a clinicopathologic study of 23 cases. Am J Surg Pathol 1982; 6:631–637.

86. Murphey MD, Robbin MR, McRae GA, Flemming DJ, Temple T, Kransdorf MJ. The many faces of osteosarcoma. RadioGraphics 1997; 17: 1205–1232.
87. Unni KK, Dahlin DC, Beabout JW. Periosteal osteogenic sarcoma. Cancer 1976; 37:2476–2485.
88. Hall RB, Robinson LH, Malawar MM, Dunham WK. Periosteal osteosarcoma. Cancer 1985; 55: 165–171.
89. Kilpatrick SE, Inwards CY, Fletcher CD, Smith MA, Gitelis S. Myxoid chondrosarcoma (chordoid sarcoma) of bone: a report of two cases and review of the literature. Cancer 1997; 79:1903–1910.
90. Steiner G, Greenspan A, Jahss M, Norman A. Myxoid chondrosarcoma of the os calcis: a case report. Foot Ankle 1984; 5:84–91.
91. Martinez-Tello FJ, Navas-Palacios JJ. Ultrastructural study of conventional chondrosarcomas and myxoid- and mesenchymal-chondrosarcomas. Virchows Arch A Pathol Anat Histol 1982; 396: 197–211.
92. Fu YS, Kay S. A comparative ultrastructural study of mesenchymal chondrosarcoma and myxoid chondrosarcoma. Cancer 1974; 33:1531–1542.
93. Gill S, McManus AP, Crew AJ, et al. Fusion of the EWS gene to a DNA segment from 9q22-31 in a human myxoid chondrosarcoma. Genes Chromosomes Cancer 1995; 12:307–310.
94. Sjogren H, Meis-Kindblom JM, Orndal C, et al. Studies on the molecular pathogenesis of extraskeletal myxoid chondrosarcoma: cytogenetic, molecular genetic, and cDNA microarray analyses. Am J Pathol 2003; 162:781–792.
95. Lichtenstein L, Bernstein D. Unusual benign and malignant chondroid tumors of bone. Cancer 1959; 12:1142–1157.
96. Nakashima Y, Unni KK, Shives TC, Swee RG, Dahlin DC. Mesenchymal chondrosarcoma of bone and soft tissue: a review of 111 cases. Cancer 1986; 57:2444–2453.
97. Blackwell JB. Mesenchymal chondrosarcoma arising in fibrous dysplasia of the femur. J Clin Pathol 1993; 46:961–962.
98. Leggon RE, Munro M, Schuerch C. Thigh mass in a 52-year-old woman. Clin Orthop Rel Res 2001; 388:252–263.
99. Shapeero LG, Vanel D, Couanet D, Contesso G, Ackerman LV. Extraskeletal mesenchymal chondrosarcoma. Radiology 1993; 186:819–826.
100. Koeller KK. Mesencymal chondrosarcoma and simulating lesions of the orbit. Radiol Clin North Am 1999; 37:203–217.
101. Salvador AH, Beabout JW, Dahlin DC. Mesenchymal chondrosarcoma: observations on 30 new cases. Cancer 1971; 28:605–615.
102. Shinaver CN, Mafee MF, Choi KH. MRI of mesenchymal chondrosarcoma of the orbit: case report and review of the literature. Neuroradiol 1997; 39:296–301.
103. Ly JQ. Mesenchymal chondrosarcoma of the maxilla. AJR Am J Roentgenol 2002; 179:1077–1078.
104. Bloem JL, Reiser MF, Vanel D. Magnetic resonance contrast agents in the evaluation of the musculoskeletal system. Magn Reson Q 1990; 6:136–163.
105. Kransdorf MJ. Malignant soft-tissue tumors in a large referral population: distribution of diagnoses by age, sex and location. AJR Am J Roentgenol 1995; 164:129–134.
106. Weiss SW, Goldblum JR. Cartilaginous soft tissue tumors. In: Strauss M, ed. Enzinger and Weiss's soft tissue tumors. 4th ed. St Louis, Mo: Mosby, 2001; 1368–1388.
107. Miettinen M. Cartilage and bone-forming tumors and tumor-like lesions. In: Diagnostic soft tissue pathology. Philadelphia, Pa: Churchill-Livingstone, 2003; 407–409.
108. Enzinger FM, Shiraki M. Extraskeletal myxoid chondrosarcoma: an analysis of 34 cases. Hum Pathol 1972; 3:421–435.
109. Whitten CG, El-Khoury GY, Benda JA, Ehara S. Case report 829: intramuscular myxoid chondrosarcoma. Skeletal Radiol 1994; 23:153–156.
110. Kransdorf MJ, Meis JM. Extraskeletal osseous and cartilaginous tumors of the extremities. RadioGraphics 1993; 13:853–884.
111. Meis JM, Martz KL. Extraskeletal myxoid chondrosarcoma: a clinicopathologic study of 120 cases (abstr). Lab Invest 1992; 66:9A.
112. Saleh G, Evans HL, Ro JY, Ayala AG. Extraskeletal myxoid chondrosarcoma: a clinicopathologic study of ten patients with long-term follow-up. Cancer 1992; 70:2827–2830.
113. Kawaguchi S, Wada T, Nagoya S, et al. Extraskeletal myxoid chondrosarcoma: a multi-institutional study of 42 cases in Japan. Cancer 2003; 97:1285–1292.
114. Goldenberg RR, Cohen P, Steinlauf P. Chondrosarcoma of the extraskeletal soft tissues. J Bone Joint Surg Am 1967; 49:1487–1507.
115. Harwood AR, Krajbich JI, Fornasier VL. Mesenchymal chondrosarcoma: a report of 17 cases. Clin Orthop Rel Res 1981; 158:144–148.
116. Chhem RK, Bui BT, Calderon-Villar H, Fontaine S. Case report: primary mesenchymal chondrosarcoma of the brain. Clin Radiol 1992; 45: 422–423.
117. Dahlin DC, Beabout JW. Dedifferentiation of low-grade chondrosarcomas. Cancer 1971; 28: 461–466.
118. Anract P, Tomeno B, Forest M. Dedifferentiated chondrosarcoma: a study of 13 clinical cases and review of the literature. Rev Chir Orthop Reparatrice Appar Mot 1994; 80:669–680. [French]
119. Campanacci M, Bertoni F, Capanna R. Dedifferentiated chondrosarcomas. Ital J Orthop Traumatol 1979; 5:331–341.
120. Capanna R, Bertoni F, Bettelli G, et al. Dedifferentiated chondrosarcoma. J Bone Joint Surg Am 1988; 70:60–69.
121. Daly PJ, Sim FH, Wold LE. Dedifferentiated chondrosarcoma of bone. Orthopedics 1989; 12: 763–767.
122. Frassica FJ, Unni KK, Beabout JW, et al. Dedifferentiated chondrosarcoma: a report of the clinicopathological feature and treatment of seventy-eight cases. J Bone Joint Surg Am 1986; 68: 1197–1205.
123. Mercuri M, Picci P, Campanacci L, Rulli E. Dedifferentiated chondrosarcoma. Skeletal Radiol 1995; 24:409–416.

124. Mankin HL, Cantley KP, Lippiello L, Schille AL, Campbell CJ. The biology of human chondrosarcoma. I. Description of cases, grading, and biochemical analyses. J Bone Joint Surg Am 1980; 62:160–176.
125. Mankin HL, Cantley KP, Lippiello L, Schille AL, Campbell CJ. The biology of human chondrosarcoma. II. Variation in chemical composition among types and subtypes of benign and malignant cartilage tumors. J Bone Joint Surg Am 1980; 62:176–188.
126. Schreuder HW, Keijser LC, Veth RP. Beneficial effects of cryosurgery treatment in benign and low-grade-malignant bone tumors in 120 patients. Ned Tijdschr Geneeskd 1999; 143:2275–2281. [Dutch]
127. Schreuder HW, Prusczynski M, Veth RP, Lemmens JA. Treament of benign and low-grade malignant intramedullary chondroid tumours with curettage and cryosurgery. Eur J Surg Oncol 1998; 24:120–126.
128. Sheth DS, Yasko AW, Johnson ME, Ayala AG, Murray JA, Romsdahl MM. Chondrosarcoma of the pelvis: prognostic factors for 67 patients treated with definitive surgery. Cancer 1996; 78: 745–750.
129. Springfield DS, Gebhardt MC, McGuire MH. Chondrosarcoma: a review. J Bone Joint Surg Am 1996; 78:141–149.
130. Gitelis S, Bertoni F, Picci CP, Campanacci M. Chondrosarcoma of bone. J Bone Joint Surg Am 1981; 63:1248–1256.
131. Mitchell A, Rudan JR, Fenton PV. Juxtacortical dedifferentiated chondrosarcoma from a primary periosteal chondrosarcoma. Mod Pathol 1996; 9:279–283.
132. Mitchell AD, Ayoub K, Mangham DC, Grimer RJ, Carter SR, Tillman RM. Experience in the treatment of dedifferentiated chondrosarcoma. J Bone Joint Surg Br 2000; 82:55–61.
133. Harwood AR, Krajbich JI, Fornasier VL. Radiotherapy of chondrosarcoma of bone. Cancer 1980; 45:2769–2777.
134. Multhaupt HA, Alvarez JC, Rafferty PA, Warhol MJ, Lackman RD. Fluoroquinolone's effect on growth of human chondrocytes and chondrosarcomas: in vitro and in vivo correlation. J Bone Joint Surg Am 2001; 83:56–61.

This article meets the criteria for 1.0 credit hour in category 1 of the AMA Physician's Recognition Award. To obtain credit, see accompanying test at http://www.rsna.org/education/rg_cme.html.